On a multiscale model involving cell contractivity and its effects on tumor invasion

Gülnihal Meral[1], Christian Stinner[2]*, Christina Surulescu[2]
[1] Bülent Ecevit University, Faculty of Arts and Sciences, Department of Mathematics, 67100 Zonguldak, Turkey
[2] Technische Universität Kaiserslautern, Felix-Klein-Zentrum für Mathematik, Paul-Ehrlich-Str. 31, 67663 Kaiserslautern, Germany
E-Mail: gulnihal.meral@beun.edu.tr, stinner,surulescu@mathematik.uni-kl.de

Abstract

Cancer cell migration is an essential feature in the process of tumor spread and establishing of metastasis. It characterizes the invasion observed on the level of the cell population, but it is also tightly connected to the events taking place on the subcellular level. These are conditioning the motile and proliferative behavior of the cells, but are also influenced by it. In this work we propose a multiscale model linking these two levels and aiming to assess their interdependence. On the subcellular, microscopic scale it accounts for integrin binding to soluble and insoluble components present in the peritumoral environment, which is seen as the onset of biochemical events leading to changes in the cell's ability to contract and modify its shape. On the macroscale of the cell population this leads to modifications in the diffusion and haptotaxis performed by the tumor cells and implicitly to changes in the tumor environment. We prove the (local) well posedness of our model and perform numerical simulations in order to illustrate the model predictions.

Key words: multiscale models, cancer cell migration, reaction-diffusion-transport equations, delay differential equations, chemotaxis, haptotaxis
MSC 2010: 35Q92, 92C17, 35K57

1 Introduction

Tumor cells are able to migrate through the surrounding tissue and degrade it on their way toward blood vessels and distal organs where they initiate and develop further tumors, a process known as metastasis [14]. According to the structure of the peritumoral environment, the movement of cancer cells is diffusion- or transport-dominated and also influenced by two mechanisms: *chemotaxis* and *haptotaxis*. The former defines the cell motion in response to a chemoattractant (or chemorepellent) concentration. As such gradients may lack in the solution, the differences in the concentration of an adhesive molecule e.g., along an extracellular matrix (ECM) can be relevant instead. The cells need to adhere to the ECM fibers in order to be able to move [1], hence they will migrate from a region of low concentration of relevant adhesive molecules to an area with a higher concentration, a process called *haptotaxis* [7]. Thereby, the contact with the surrounding tissue stimulates

*corresponding author

the production of proteolytic enzymes (matrix degrading enzymes (MDEs) like matrix metalloproteinases), which degrade the tissue fibers [15], thus creating interstices to be occupied during the migration process toward neighboring blood vessels.

When characterizing tumor migration, the spatial scales of interest range from the subcellular level to the macroscopic one (tissue and cell populations), while the time scales stretch from seconds (or even shorter) at the intracellular level up to months for the doubling times of tumors.

Most of the existing models for cancer invasion can be assigned to three categories:

Microscopic models are concerned with the events at the subcellular level initiating and controling (tumor) cell migration. These processes are usually characterized with systems of ordinary differential equations (ODEs) for the concentrations of the involved biochemical substances. For instance, some of these models focus on the expression of MDEs and proteolysis [6], whereas others emphasize cell polarization and onset of lamellipod protrusion [24], a crucial step in integrin-mediated haptotactic motility.

In the *mesoscopic framework*, cell migration is characterized by Boltzmann-like kinetic transport equations for the cell density function, in which the integral operators characterize innovations of the cell velocities instead of modeling particle collisions as in gas theory. This approach has been introduced by Othmer, Dunbar & Alt [28] in order to provide a description of cell dispersal via velocity jump processes. It was extended e.g., by Hillen [17] to model the mesenchymal motion of cancer cells and the subsequent tissue modification. Bellomo et al. [5] proposed a general framework for such kinetic models on the mesoscopic level (also allowing for the inclusion of the "cell state" to reflect dynamics on the microlevel) that they called the *kinetic theory of active particles* (KTAP).

Macroscopic descriptions can be derived from mesoscopic models by means of averaging processes leading to evolution equations for the moments of the cell distribution function. This was done, at least formally, in, e.g., [17] in the context of mesenchymal motion of tumor cells, whereas rigorous results on hyperbolic and parabolic limits of kinetic equations for chemotaxis were obtained, e.g., in [8] and [29] respectively. Further models for cell population migration that rely only on mass balance equations were proposed by Anderson et al. [2] and Chaplain & Lolas [9], for example.

Combining two or all three of these modeling levels leads to a *multiscale setting*, which has received increasing interest over the last decade. Many – in particular those involving couplings between micro and mesoscales – align to the general KTAP by Bellomo et al. In [32, 20, 21] multiscale models for bacterial dispersal and respectively for cancer cell migration through tissue networks have been deduced and analyzed. On the subcellular level the latter account for integrin binding to ECM fibers or to proteolytic rests resulting from the degradation of such fibers, whereas the behavior of individual cells on the mesoscopic scale is described via a Boltzmann-type transport equation for the cell density function. This in turn is further coupled with an integro-differential ODE for the ECM fiber density and a reaction-diffusion equation (RD-PDE) for the chemoattractant concentration. Bridging the gap between the scales, the macroscopic fiber density influences the vector field of subcellular states. A related model for glioma invasion focusing on haptotaxis and the interaction between tumor cells and brain tissue via integrin binding on the microlevel was studied in [12]. Due to its high dimensionality and the large differences between the scales, the numerical handling of such a micro-meso-macro model is a challenging issue. A way out is to use adequate scalings to obtain macroscopic limits, as in [12, 34]. An-

other way uses a nonparametric density estimation technique from statistics to assess the density of cells directly on the macrolevel, without needing to deduce the corresponding reaction-diffusion (transport) equations (RD(T)-PDEs), but only relying on simulations of the involved basic stochastic processes [30, 31, 32].

Yet another way to avoid the difficulties with the numerics of a full micro-meso-macro model is to directly connect the microscopic and the macroscopic levels, leading to a much simplified (but still multiscale) approach, which concentrates on the population evolution at the macroscopic level and uses systems of RD(T)-PDEs. These are coupled with ODEs modeling processes inside or on the surface of a cell. The coefficients in the macroscopic formulation (for, e.g., diffusion, chemotaxis, haptotaxis) can depend in a nonlinear way on the solutions and even on the microscale dynamics. In this work we use such an approach: motivated by the more complex micro-meso-macro setting in [20, 21] we propose a micro-macro model for the influence of integrin binding dynamics on tumor invasion by way of a contractivity function. The latter captures the effects of subcellular dynamics on the ability of a cell to polarize and modify its shape by restructuring its cytoskeleton. The integrins on the cell surface bind (reversibly) to insoluble (ECM fibers) and soluble (proteolytic rests of ECM fibers) ligands which are present in the peritumoral environment, hence initiating a whole network of intracellular signaling cascades (see e.g., [23] and the references therein), the outcome of which are – as already mentioned – changes in the cell's flexibility. These, however, are expected to need some time to happen, which is modeled by a time lag in the equation characterizing the evolution of the contractivity function. Further, these events on the subcellular level have consequences for the cell's migratory behavior, influencing both its diffusive spread and the haptotaxis, which we model by letting the respective coefficients depend on the cell contractivity function, see equation (2.5) below.

The paper has the following structure: In Section 2 we introduce our multiscale model characterizing the evolution of cancer cell density, concentration of proteolytic rests, density of tissue fibers, contractivity function, and concentrations of integrins bound to ECM fibers and to fiber residuals degraded during the interaction with tumor cells. The proof of the existence and uniqueness of a solution to this system is done in Section 3, followed in Section 4 by a nondimensionalization preliminary to the numerical simulations performed in Section 5. Finally, a discussion of the results is provided in Section 6.

2 The Model

2.1 The subcellular level

We provide a simplified description of the events on the subcellular level by considering as in [20, 21, 25] merely the integrin binding dynamics on the cell surface. For the sake of completeness we recall here the corresponding kinetic model for the binding of ECM-proteins v and proteolytic products l to free integrins denoted by R. The reversible binding of integrins to ECM-proteins leads to a complex Rv according to the equation

$$v + R \underset{k_{-1}}{\overset{k_1}{\rightleftharpoons}} Rv.$$

The corresponding equation for the formation and dissociation of complexes Rl of integrin and proteolytic product reads

$$l + R \underset{k_{-2}}{\overset{k_2}{\rightleftharpoons}} Rl.$$

We denote the concentrations of integrins of an individual cell bound to ECM-molecules by y_1 and the concentration of integrins of the same cell bound to the proteolytic product l by y_2. The total concentration of integrins (bound or unbound) of each cell is assumed to be conserved and given by $R_0 \in \mathbb{R}_+$. Thus, $R_0 - y_1 - y_2$ is the concentration of unbound integrins on the cell's surface. Hence, one has $\boldsymbol{y} = (y_1, y_2) \in Y$ with

$$Y := \{(y_1, y_2) \in (0, R_0)^2 \mid y_1 + y_2 < R_0\}. \tag{2.1}$$

The state equations for the cell surface dynamics then read

$$\frac{\partial \boldsymbol{y}}{\partial t} = \boldsymbol{G}(\boldsymbol{y}, v(t, \boldsymbol{x}), l(t, \boldsymbol{x})) \tag{2.2}$$

with the mapping $\boldsymbol{G} : Y \times [0, \infty) \times [0, \infty) \to \mathbb{R}^2$ defined by

$$\boldsymbol{G}(\boldsymbol{y}, v, l) := \begin{pmatrix} k_1(R_0 - y_1 - y_2)v - k_{-1}y_1 \\ k_2(R_0 - y_1 - y_2)l - k_{-2}y_2 \end{pmatrix}. \tag{2.3}$$

On the other hand, since contractivity is the outcome of a sequence of biochemical processes initiated by binding of integrins, activation of multiple signaling proteins and involving e.g., actin polimerization, restructuring of the cell's cytoskeleton, formation of protrusions, polarization etc. (see e.g., [19] and the references therein), it is reasonable to assume that it depends on some delay corresponding to the time passed between integrin binding and the effects on the cell's ability to reorganize its shape by contraction. This leads to an equation of the form

$$\kappa_t = -q\kappa + H(\boldsymbol{y}(t - \tau)) \qquad \text{in } (0, T) \times \Omega \tag{2.4}$$

with τ denoting the fixed delay in taking influence on the contractivity. Another choice for the time lag is to use a distributed one, as in the next section.

2.2 The macroscopic level

The evolution of cancer cell density $c(t, \boldsymbol{x})$ is influenced by the random motility $\mathbf{J_{random}}$ and the directional flow $\mathbf{J_{directional}}$. The former characterizes cell diffusion into the tissue and is given by

$$\mathbf{J_{random}} = -\varphi(\kappa, c, v)\nabla c$$

with the random motility function $\varphi(\kappa, c, v)$ depending on the contractivity function κ, on the cell density itself, and on the density $v(t, \boldsymbol{x})$ of tissue fibers, as the spread of cancer cells is conditioned by their neighbors and surroundings.
On the other hand, $\mathbf{J_{directional}}$ corresponds to the cancer cell flux due to spatial gradients of stimulating chemotactic and haptotactic responses:

$$\mathbf{J_{directional}} = \mathbf{J_{chemotaxis}} + \mathbf{J_{haptotaxis}} = f(c, l)c\nabla l + \psi(\kappa, v)c\nabla v$$

where $f(c,l)$ and $\psi(\kappa,v)$ are the chemotactic and haptotactic functions, respectively. As in [20, 21, 25], in our present model the role of the chemoattractant is played by the proteolytic residuals following the degradation of tissue by the cells performing mesenchymal motion [13, 18]. We denote with $l(t,\boldsymbol{x})$ their concentration.
Then, due to the equilibrium of fluxes we obtain the first equation in system (2.5) below. Thereby, the last term on the right-hand side models cell proliferation with crowding effects and the proliferation rate and the carrying capacity are denoted by μ_c and K_c, respectively.
The ECM fibers are supposed to be degraded through interaction with the cancer cells with the rate δ_v. They also reestablish and remodel themselves while competing with the diffusive cancer cells for space. This is described by a term similar to the proliferation in the equation for cancer cells with the corresponding production rate μ_v and carrying capacity K_v. Crowding effects are accounted for as well. Further, the ECM does not diffuse, but can be only degraded by the cells producing matrix degrading enzymes. These considerations lead to the second equation in system (2.5).
The chemoattractant concentration satisfies a reaction-diffusion equation with a source term reflecting the degradation of tissue fibers under the influence of the migrating tumor cells, along with a simple decay term. The diffusion constant, production and decay rates are denoted with α, δ_l and β, respectively.
Finally combining the equations on micro and macro levels, we obtain the following system of equations:

$$\begin{cases} c_t = \nabla\cdot(\varphi(\kappa,c,v)\nabla c) - \nabla\cdot(\psi(\kappa,v)c\nabla v) - \nabla\cdot(f(c,l)c\nabla l) \\ \qquad +\mu_c c\left(1-\frac{c}{K_c}-\eta_1\frac{v}{K_v}\right), \\ v_t = -\delta_v cv + \mu_v v\left(1-\eta_2\frac{c}{K_c}-\frac{v}{K_v}\right), \\ l_t = \alpha\Delta l + \delta_l cv - \beta l, \\ \boldsymbol{y}_t = \boldsymbol{G}(v,l,\boldsymbol{y}), \\ \kappa_t = -q\kappa + H(\boldsymbol{y}(t-\tau)) \end{cases} \tag{2.5}$$

in $(0,T)\times\Omega$, where $\Omega\subset\mathbb{R}^n$ is a bounded domain with a smooth enough boundary and with $n\in\{1,2,3\}$. Here $\eta_1,\eta_2\in(0,1)$ are parameters characterizing growth reduction due to the competition between the cancer cells and the tissue fibers (see e.g., [16]).
We further assume the boundary conditions

$$\frac{\partial c}{\partial\boldsymbol{\nu}} = \frac{\partial v}{\partial\boldsymbol{\nu}} = \frac{\partial l}{\partial\boldsymbol{\nu}} = 0 \qquad \text{on } (0,T)\times\partial\Omega, \tag{2.6}$$

where $\boldsymbol{\nu}$ denotes the outward unit normal vector on $\partial\Omega$, and the initial conditions

$$\begin{aligned} &c(0,\boldsymbol{x}) = c_0(\boldsymbol{x}), \quad v(0,\boldsymbol{x}) = v_0(\boldsymbol{x}), \quad l(0,\boldsymbol{x}) = l_0(\boldsymbol{x}), \\ &\kappa(0,\boldsymbol{x}) = \kappa_0(\boldsymbol{x}), \quad \boldsymbol{y}(t,\boldsymbol{x}) = \boldsymbol{y}_0(\boldsymbol{x}), \end{aligned} \qquad t\in(-\infty,0], \quad \boldsymbol{x}\in\Omega. \tag{2.7}$$

In our model we consider

$$\varphi(\kappa,c,v) = \frac{D_c\kappa}{1+\frac{cv}{K_cK_v}},\ \psi(\kappa,v) = \frac{D_H\kappa v}{K_v+v},\ f(c,l) = \frac{D_k}{1+\frac{cl}{K_cl_0}},\ H(\boldsymbol{y}) = \frac{My_1}{R_0+y_2} \tag{2.8}$$

for the random motility, haptotaxis and chemotaxis functions and for the function modeling the influence of the integrin binding on the contractivity, respectively. Here K_c and K_v are the carrying capacities for the cancer cells and ECM, respectively, and l_0 is an appropriate reference variable for the proteolytic rests.

3 Local Existence

3.1 The case with distributed delay

In this case we start by considering a distributed delay

$$\kappa(t,\boldsymbol{x}) = \int_0^\infty q e^{-qu} \tilde{H}(\boldsymbol{y}(t-u,\boldsymbol{x}))\,du, \qquad (t,\boldsymbol{x}) \in (0,T)\times\Omega, \tag{3.1}$$

for the characterization of the cell contractivity. Using the transformation $s = t-u$, (3.1) is equivalent to

$$\kappa(t,\boldsymbol{x}) = \int_{-\infty}^t q e^{-q(t-s)} \tilde{H}(\boldsymbol{y}(s,\boldsymbol{x}))\,ds, \qquad (t,\boldsymbol{x}) \in (0,T)\times\Omega.$$

In view of (2.7) this means that κ fulfills (2.4) with $\tau = 0$, $H(\boldsymbol{y}) := q\tilde{H}(\boldsymbol{y})$ and the initial condition

$$\kappa(0,\boldsymbol{x}) = \int_{-\infty}^0 q e^{qs} \tilde{H}(\boldsymbol{y}_0(\boldsymbol{x}))\,ds = \tilde{H}(\boldsymbol{y}_0(\boldsymbol{x})) =: \kappa_0(\boldsymbol{x}), \qquad \boldsymbol{x}\in\Omega.$$

Hence, the distributed delay corresponds to the case $\tau = 0$ for the problem (2.5)-(2.7).

Thus, we fix $\tau = 0$, $p \in (\frac{n+2}{2},\infty)$ and define the spaces

$$\begin{aligned} X &:= \left\{u \in L^p(0,T;W^{2,p}(\Omega)) \,:\, u_t \in L^p(0,T;L^p(\Omega))\right\},\\ Z &:= L^{2p}(0,T;W^{1,2p}(\Omega)), \qquad V := C^1(0,T;C^0(\bar\Omega)). \end{aligned}$$

Then we have the following local existence result for the case with distributed delay.

Theorem 3.1 *Assume $\tau = 0$, $p \in (\frac{n+2}{2},\infty)$,*

$$\begin{aligned} &c_0, v_0, l_0 \in W^{2,p}(\Omega),\ \kappa_0 \in W^{1,2p}(\Omega),\ \boldsymbol{y}_0 \in (W^{1,2p}(\Omega))^2,\ \tfrac{\partial c_0}{\partial \boldsymbol{\nu}} = \tfrac{\partial v_0}{\partial \boldsymbol{\nu}} = \tfrac{\partial l_0}{\partial \boldsymbol{\nu}} = 0\\ &\text{on } \partial\Omega, \quad 0 < c_0 < K_c,\ 0 < v_0 < K_v,\ l_0 > 0,\ \kappa_0 > 0 \text{ and } \boldsymbol{y}_0 \in Y \text{ for all } \boldsymbol{x}\in\bar\Omega \end{aligned} \tag{3.2}$$

together with (2.3) *and let*

$$\begin{aligned} &H \in C^1(\bar Y), f \in C^1([0,\infty)^2), \varphi \in C^1([0,\infty)^3), \psi \in C^1([0,\infty)^2) \text{ be nonnegative}\\ &\text{such that for any } 0 < a < b < \infty \text{ there exists } \delta_{a,b} > 0 \text{ with}\\ &\varphi(\kappa,c,v) \ge \delta_{a,b} \text{ for all } (\kappa,c,v) \in [a,b]\times[0,\infty)^2. \end{aligned} \tag{3.3}$$

Then there is $T > 0$ such that there exists a unique solution to (2.5)-(2.7) *satisfying*

$$\begin{aligned} &c, l \in X,\ v \in X\cap V,\ \kappa \in Z\cap V,\ \boldsymbol{y} \in Z^2 \cap V^2 \text{ such that}\\ &0 \le c \le K_c,\ 0 < v \le K_v,\ l \ge 0,\ \kappa > 0 \text{ and } \boldsymbol{y} \in Y \text{ for all } (t,\boldsymbol{x}) \in [0,T)\times\bar\Omega. \end{aligned} \tag{3.4}$$

Proof. We define

$$X_0 := \left\{c \in X \,:\, c \ge 0,\ \|c\|_X \le \gamma := \|c_0\|_{W^{2,p}(\Omega)} + 1,\ \frac{\partial c}{\partial \boldsymbol{\nu}} = 0 \text{ on } (0,T)\times\partial\Omega\right\},$$

fix $T_0 \in (0,\infty)$ such that $c_0 \in X_0$ for all $T \in (0,T_0]$ and define the map $\mathcal{F} : X_0 \to X_0$ with $\mathcal{F}(\tilde{c}) = c$, where c is defined in the following way: Given $\tilde{c} \in X_0$, we let v, l, κ, $\boldsymbol{y}$ and c denote the solutions of the problems

$$\begin{cases} v_t = -\delta_v \tilde{c} v + \mu_v v \left(1 - \eta_2 \frac{\tilde{c}}{K_c} - \frac{v}{K_v}\right) & \text{in } (0,T)\times\Omega, \\ v(0,\boldsymbol{x}) = v_0(\boldsymbol{x}) & \text{in } \Omega, \end{cases} \tag{3.5}$$

$$\begin{cases} l_t = \alpha \Delta l + \delta_l \tilde{c} v - \beta l & \text{in } (0,T)\times\Omega, \\ \frac{\partial l}{\partial \boldsymbol{\nu}} = 0 & \text{on } (0,T)\times\partial\Omega, \\ l(0,\boldsymbol{x}) = l_0(\boldsymbol{x}) & \text{in } \Omega, \end{cases} \tag{3.6}$$

$$\begin{cases} \boldsymbol{y}_t = \boldsymbol{G}(v,l,\boldsymbol{y}) & \text{in } (0,T)\times\Omega, \\ \boldsymbol{y}(0,\boldsymbol{x}) = \boldsymbol{y}_0(\boldsymbol{x}) & \text{in } \Omega, \end{cases} \tag{3.7}$$

$$\begin{cases} \kappa_t = -q\kappa + H(\boldsymbol{y}(t)) & \text{in } (0,T)\times\Omega, \\ \kappa(0,\boldsymbol{x}) = \kappa_0(\boldsymbol{x}) & \text{in } \Omega, \end{cases} \tag{3.8}$$

$$\begin{cases} c_t = \nabla\cdot(\varphi(\kappa,\tilde{c},v)\nabla c) - \nabla\cdot(\psi(\kappa,v)c\nabla v) - \nabla\cdot(f(\tilde{c},l)c\nabla l) \\ \qquad +\mu_c c\left(1 - \frac{\tilde{c}}{K_c} - \eta_1\frac{v}{K_v}\right) & \text{in } (0,T)\times\Omega, \\ \frac{\partial c}{\partial \boldsymbol{\nu}} = 0 & \text{on } (0,T)\times\partial\Omega, \\ c(0,\boldsymbol{x}) = c_0(\boldsymbol{x}) & \text{in } \Omega. \end{cases} \tag{3.9}$$

In order to obtain a unique solution of (2.5)-(2.7) for $T \in (0,T_0]$ small enough, we proceed in several steps.

Step 1: Estimates
For given $\tilde{c} \in X_0$, (3.5) is an ODE of Bernoulli type which is explicitly solvable. Using (3.2) along with the nonnegativity of $\tilde{c}$, an ODE comparison principle implies that

$$0 \le v \le K_v \qquad \text{in } [0,T]\times\bar{\Omega} \tag{3.10}$$

is fulfilled, since 0 and K_v are constant sub- and supersolutions to (3.5), respectively. As X is continuously embedded into $C^0([0,T]\times\bar{\Omega})$ (see [22, Lemma II.3.3]) and $\|\tilde{c}\|_X \le \gamma$, we obtain from (3.10) that $v_t \ge -C_1 v$ with some $C_1 > 0$ depending on γ. In view of $T \le T_0$ and (3.2) this implies

$$v(t,\boldsymbol{x}) \ge e^{-C_1 T_0}\left(\min_{\boldsymbol{x}\in\bar{\Omega}} v_0(\boldsymbol{x})\right) =: C_2 > 0, \qquad (t,\boldsymbol{x}) \in (0,T)\times\Omega. \tag{3.11}$$

Hence, $z := \frac{1}{v}$ is uniformly bounded in $(0,T)\times\Omega$ and satisfies the linear ODE

$$z_t = \left(-\mu_v + \tilde{c}\left(\delta_v + \eta_2\frac{\mu_v}{K_c}\right)\right) z + \frac{\mu_v}{K_v} \qquad \text{in } (0,T)\times\Omega. \tag{3.12}$$

In view of (3.2), (3.10), (3.11) and $\tilde{c} \in X_0$, we therefore conclude that v fulfills

$$C_2 \le v \le K_v \quad \text{in } [0,T]\times\bar{\Omega}, \qquad \|v\|_X + \|v\|_V \le C_3, \qquad \frac{\partial v}{\partial \boldsymbol{\nu}} = 0 \quad \text{on } (0,T)\times\partial\Omega \tag{3.13}$$

with some C_3 depending on γ and T_0, where $v \in V$ as $\tilde{c}, c_0$ are continuous due to $p > \frac{n+2}{2}$ and v_t is continuous and uniformly bounded by (3.5).

In view of $\tilde{c} \in X_0$ and (3.13), we have that $\tilde{c}v$ is uniformly bounded in $(0,T)\times\Omega$. Hence, by [22, Theorem IV.9.1] (and the remark at the end of Section IV.9 concerning the Neumann problem) there is a unique solution l of (3.6) which satisfies

$$l \geq 0 \quad \text{in } (0,T)\times\Omega \qquad \text{and} \qquad \|l\|_X \leq C_4 \tag{3.14}$$

with some C_4 depending on γ and T_0, where the nonnegativity of l follows from the comparison principle and the nonnegativity of $\tilde{c}$, v and l_0.

Now (3.7) is a linear ODE for $\boldsymbol{y}$. As furthermore $\boldsymbol{G}$ satisfies the subtangential condition with respect to Y for all nonnegative v and l, we obtain that Y is a positive invariant set for (3.7). Thus, in view of (3.2), (3.13) and (3.14) we deduce that there is a unique solution $\boldsymbol{y}$ of (3.7) such that

$$\boldsymbol{y}(t,\boldsymbol{x}) \in Y \quad \text{for } (t,\boldsymbol{x}) \in [0,T]\times\bar{\Omega} \qquad \text{and} \qquad \|\boldsymbol{y}\|_{Z^2} + \|\boldsymbol{y}\|_{V^2} \leq C_5 \tag{3.15}$$

hold with some constant C_5 depending on γ and T_0, since X is continuously embedded into Z and $C^0([0,T]\times\bar{\Omega})$ due to $p > \frac{n+2}{2}$ (see [22, Lemma II.3.3]) and as the continuity of v and l along with (3.7) imply $\boldsymbol{y} \in V^2$.

As (3.8) is a linear ODE for κ and H is nonnegative, we deduce from (3.2), (3.13)-(3.15) and the comparison principle that (3.8) has a unique solution which fulfills

$$\begin{gathered} 0 < C_6 := e^{-qT_0}\left(\min_{\boldsymbol{x}\in\bar{\Omega}} \kappa_0(\boldsymbol{x})\right) \leq \kappa(t,\boldsymbol{x}) \leq C_7 \quad \text{for } (t,\boldsymbol{x}) \in (0,T)\times\Omega, \\ \|\kappa\|_Z + \|\kappa\|_V \leq C_8 \end{gathered} \tag{3.16}$$

with some constants depending on γ and T_0, as (3.8) is a linear ODE and $H(\boldsymbol{y}) \in C^0([0,T]\times\bar{\Omega})$ and $\kappa_0 \in C^0(\bar{\Omega})$ hold in view of the continuity of H, (3.15) and the continuous embedding of $W^{1,2p}(\Omega)$ into $C^0(\bar{\Omega})$ for $p > \frac{n+2}{2}$.

Finally, (3.9) is a linear parabolic equation for c, of the form

$$c_t = a_{ii}c_{x_ix_i} + a_ic_{x_i} + ac,$$

where

$$\begin{aligned} a_{ii} &:= \varphi(\kappa,\tilde{c},v), \\ a_i &:= \frac{\partial\varphi}{\partial\kappa}(\kappa,\tilde{c},v)\kappa_{x_i} + \frac{\partial\varphi}{\partial c}(\kappa,\tilde{c},v)\tilde{c}_{x_i} + \frac{\partial\varphi}{\partial v}(\kappa,\tilde{c},v)v_{x_i} - \psi(\kappa,v)v_{x_i} - f(\tilde{c},l)l_{x_i}, \\ a &:= -\psi(\kappa,v)v_{x_ix_i} - \frac{\partial\psi}{\partial\kappa}(\kappa,v)\kappa_{x_i}v_{x_i} - \frac{\partial\psi}{\partial v}(\kappa,v)(v_{x_i})^2 - f(\tilde{c},l)l_{x_ix_i} - \frac{\partial f}{\partial c}(\tilde{c},l)\tilde{c}_{x_i}l_{x_i} \\ &\quad - \frac{\partial f}{\partial l}(\tilde{c},l)(l_{x_i})^2 + \mu_c\left(1 - \frac{\tilde{c}}{K_c} - \eta_1\frac{v}{K_v}\right). \end{aligned}$$

In view of (3.3) and (3.13)-(3.16) and due to the continuous embedding of X into Z, a_{ii} is continuous in $[0,T]\times\bar{\Omega}$ and there are positive constants C_9 and C_{10} depending on γ and T_0 such that

$$C_9 \leq a_{ii} \leq C_{10} \quad \text{for } (t,\boldsymbol{x}) \in [0,T]\times\bar{\Omega}, \qquad \|a_i\|_{L^{2p}((0,T)\times\Omega)} + \|a\|_{L^p((0,T)\times\Omega)} \leq C_{10}. \tag{3.17}$$

Hence, by Theorem IV.9.1, its proof and the remark at the end of Section IV.9 in [22], there is some $T_1 \leq T_0$ such that for any $T \in (0, T_1]$ there is a unique solution c of (3.9) fulfilling

$$\|c\|_X \leq \|c_0\|_{W^{2,p}(\Omega)} + \varepsilon(T), \tag{3.18}$$

where $\varepsilon(T) \to 0$ as $T \searrow 0$. Hence, there exists $T_2 \in (0, T_1]$ such that $\|c\|_X \leq \gamma$ for all $T \in (0, T_2]$. As c satisfies the boundary condition (2.6) and the comparison principle implies $c \geq 0$ in $(0,T)\times\Omega$, we conclude that $\mathcal{F}$ is a well-defined self-mapping for $T \in (0, T_2]$.

Step 2: Existence
For $m \geq 1$ let v_m, l_m, $\boldsymbol{y}_m$, κ_m and c_m denote the solutions to (3.5)-(3.9) with $\tilde{c} := c_{m-1}$. In particular, we have $c_m = \mathcal{F}(c_{m-1})$. Due to Step 1, we have $\|c_m\|_X \leq \gamma$ for all $m \in \mathbb{N}$. As $X = L^p(0,T;W^{2,p}(\Omega)) \cap W^{1,p}(0,T;L^p(\Omega))$ is reflexive, X is continuously embedded into $C^\alpha([0,T]\times\bar{\Omega})$ for $0 < \alpha < 1 - \frac{n+2}{2p}$ (see [22, Lemma II.3.3]) and X is compactly embedded into $L^p(0,T;W^{1,2p}(\Omega))$ due to $p > \frac{n+2}{2}$ and the Aubin-Lions lemma (see [33, Theorem III.2.1]). Hence, there exists a subsequence of $(c_m)_{m\in\mathbb{N}}$ (not relabeled) and $c \in X$ such that

$$\begin{gathered} c_m \rightharpoonup c \text{ weakly in } X, \\ c_m \to c \text{ strongly in } L^p(0,T;W^{1,2p}(\Omega)) \text{ and in } C^0([0,T]\times\bar{\Omega}) \end{gathered} \tag{3.19}$$

for $m \to \infty$. In particular, as X is continuously embedded into Z, we have

$$\nabla c_m \to \nabla c \text{ a.e. in } (0,T)\times\Omega \quad \text{and} \quad \nabla c_m \rightharpoonup \nabla c \text{ weakly in } L^{2p}((0,T)\times\Omega) \tag{3.20}$$

for $m \to \infty$ up to a further choice of a subsequence.

In a similar way, since v_m fulfills (3.13) for all $m \in \mathbb{N}$, there is a subsequence such that

$$\begin{gathered} v_m \rightharpoonup v \text{ weakly in } X, \\ v_m \to v \text{ strongly in } L^p(0,T;W^{1,2p}(\Omega)) \text{ and in } C^0([0,T]\times\bar{\Omega}), \\ \nabla v_m \to \nabla v \text{ a.e. in } (0,T)\times\Omega \quad \text{and} \quad \nabla v_m \rightharpoonup \nabla v \text{ weakly in } L^{2p}((0,T)\times\Omega) \end{gathered} \tag{3.21}$$

for $m \to \infty$. Hence, in view of (3.19) and (3.21) and as v_m solves (3.5) with $\tilde{c} = c_{m-1}$ for $m \in \mathbb{N}$, v is a solution to

$$\int_0^T \int_\Omega -v\Phi_t \, d\boldsymbol{x}dt = \int_0^T \int_\Omega \left[-\delta_v c v + \mu_v v \left(1 - \eta_2 \frac{c}{K_c} - \frac{v}{K_v}\right)\right] \Phi \, d\boldsymbol{x}dt$$

for all $\Phi \in C_0^\infty((0,T)\times\Omega)$ so that v solves the second equation of (2.5) in the weak sense. As its right-hand side is continuous in $[0,T]\times\bar{\Omega}$, we deduce that $v \in V$ is a classical solution of this equation. Due to (3.21) and (3.13), v further satisfies (2.6), (2.7) and (3.4).

Using (3.14), we obtain a further subsequence such that

$$\begin{gathered} l_m \rightharpoonup l \text{ weakly in } X, \\ l_m \to l \text{ strongly in } L^p(0,T;W^{1,2p}(\Omega)) \text{ and in } C^0([0,T]\times\bar{\Omega}), \\ \nabla l_m \to \nabla l \text{ a.e. in } (0,T)\times\Omega \quad \text{and} \quad \nabla l_m \rightharpoonup \nabla l \text{ weakly in } L^{2p}((0,T)\times\Omega) \end{gathered} \tag{3.22}$$

for $m \to \infty$. In view of (3.14) and (3.21) and since l_m satisfies (3.6) with $\tilde{c} = c_{m-1}$ for $m \in \mathbb{N}$, this implies that l is a weak solution to the third equation of (2.5) such that (2.6),

(2.7) and (3.4) are fulfilled.

Moreover, (3.15) also implies that $(\boldsymbol{y}_m)_m$ is uniformly bounded in $(W^{1,2p}((0,T)\times\Omega))^2$ and this space is compactly embedded into $(C^0([0,T]\times\bar{\Omega}))^2$, due to $p > \frac{n+2}{2}$. Thus, we can choose another subsequence such that

$$\begin{aligned} \boldsymbol{y}_m &\rightharpoonup \boldsymbol{y} \text{ weakly in } Z^2 \text{ and in } (W^{1,2p}((0,T)\times\Omega))^2, \\ \boldsymbol{y}_m &\to \boldsymbol{y} \text{ strongly in } (C^0([0,T]\times\bar{\Omega}))^2 \end{aligned} \tag{3.23}$$

for $m \to \infty$. Combined with (3.21), (3.22) and (3.7) for $m \in \mathbb{N}$, this implies that $\boldsymbol{y}$ is a weak solution to the last equation of (2.5). As its right-hand side is continuous in $[0,T]\times\bar{\Omega}$, we deduce that $\boldsymbol{y} \in V^2$ is a classical solution of this equation. Furthermore, (2.7) and (3.4) are satisfied due to (3.15).

In a similar way, by (3.16) we obtain a subsequence such that

$$\begin{aligned} \kappa_m &\rightharpoonup \kappa \text{ weakly in } Z \text{ and in } W^{1,2p}((0,T)\times\Omega), \\ \kappa_m &\to \kappa \text{ strongly in } C^0([0,T]\times\bar{\Omega}) \end{aligned} \tag{3.24}$$

for $m \to \infty$. Together with (3.23) and (3.8) for $m \in \mathbb{N}$, this implies that κ is a weak solution to (2.4). Due to the continuity in $[0,T]\times\bar{\Omega}$ of the right hand side in (2.4), we deduce that $\kappa \in V$ is a classical solution of this equation. Furthermore, (2.7) and (3.4) hold, due to (3.16).

Now c_m is a weak solution to

$$\begin{cases} \partial_t c_m = \nabla\cdot(\varphi(\kappa_m, c_{m-1}, v_m)\nabla c_m) - \nabla\cdot(\psi(\kappa_m, v_m)c_m\nabla v_m) \\ \qquad\qquad -\nabla\cdot(f(c_{m-1}, l_m)c_m\nabla l_m) + \mu_c c_m\left(1 - \frac{c_{m-1}}{K_c} - \eta_1\frac{v_m}{K_v}\right) \text{ in } (0,T)\times\Omega, \\ \frac{\partial c_m}{\partial \boldsymbol{\nu}} = 0 \qquad \text{on } (0,T)\times\partial\Omega, \end{cases} \tag{3.25}$$

which satisfies the initial condition $c_m(0,\boldsymbol{x}) = c_0(\boldsymbol{x})$ for $\boldsymbol{x} \in \Omega$ and $m \in \mathbb{N}$. Hence, by letting $m \to \infty$ in each of the integral terms involved in the weak formulation of (3.25) and by using (3.19)-(3.24), we conclude that c is a weak solution to the first equation of (2.5) such that (2.6) and (2.7) are fulfilled. In view of (3.19) and $c_m \geq 0$ we further have $c \in X \cap C^0([0,T]\times\bar{\Omega})$ and $c \geq 0$. As $c_0 < K_C$ in $\bar{\Omega}$, by choosing $T \in (0, T_2]$ small enough we have $0 \leq c \leq K_C$ in $[0,T]\times\bar{\Omega}$. Altogether, $\boldsymbol{S} := (c, v, l, \boldsymbol{y}, \kappa)$ is a solution to (2.5)-(2.7) which satisfies (3.4).

Step 3: Uniqueness
We now fix T as chosen in Step 2 and let $\boldsymbol{S}^{(j)} := (c^{(j)}, v^{(j)}, l^{(j)}, \boldsymbol{y}^{(j)}, \kappa^{(j)})$, $j \in \{1,2\}$, denote two solutions to (2.5)-(2.7) satisfying (3.4). As X is continuously embedded into Z and $L^\infty((0,T)\times\Omega)$ due to [22, Lemma II.3.3] and $p > \frac{n+2}{2}$, by (3.13)-(3.16) and (3.18), there exists $C_{11} > 0$ such that

$$\begin{aligned} &\|c^{(j)}\|_{L^\infty((0,T)\times\Omega)} + \|\nabla c^{(j)}\|_{L^{2p}((0,T)\times\Omega)} + \|v^{(j)}\|_{L^\infty((0,T)\times\Omega)} \\ &+\|\nabla v^{(j)}\|_{L^{2p}((0,T)\times\Omega)} + \|l^{(j)}\|_{L^\infty((0,T)\times\Omega)} + \|\nabla l^{(j)}\|_{L^{2p}((0,T)\times\Omega)} \\ &+\|\boldsymbol{y}^{(j)}\|_{(L^\infty((0,T)\times\Omega))^2} + \|\kappa^{(j)}\|_{L^\infty((0,T)\times\Omega)} + \|\nabla\kappa^{(j)}\|_{L^{2p}((0,T)\times\Omega)} \leq C_{11} \end{aligned} \tag{3.26}$$

is fulfilled for $j \in \{1,2\}$.

Since $z^{(j)} := \frac{1}{v^{(j)}}$ satisfies (3.12) with $\tilde{c} = c^{(j)}$, we have

$$\begin{aligned}\left(z^{(1)} - z^{(2)}\right)_t &= \left(-\mu_v + c^{(1)}\left(\delta_v + \eta_2\frac{\mu_v}{K_c}\right)\right)\left(z^{(1)} - z^{(2)}\right) \\ &\quad + \left(\delta_v + \eta_2\frac{\mu_v}{K_c}\right)\left(c^{(1)} - c^{(2)}\right) z^{(2)}\end{aligned}$$

which implies

$$\begin{aligned}\left(z^{(1)} - z^{(2)}\right)(t,\boldsymbol{x}) &= \left(\delta_v + \eta_2\frac{\mu_v}{K_c}\right)\int_0^t \exp\left(\int_s^t \left(-\mu_v + c^{(1)}(\sigma,\boldsymbol{x})\left(\delta_v + \eta_2\frac{\mu_v}{K_c}\right)\right)d\sigma\right) \\ &\quad \cdot \left[\left(c^{(1)} - c^{(2)}\right) z^{(2)}\right](s,\boldsymbol{x})\, ds \qquad (3.27)\end{aligned}$$

for $(t,\boldsymbol{x}) \in (0,T)\times\Omega$.
Hence, we deduce from (3.12), (3.13) and (3.26) that $\frac{1}{K_v} \le z^{(j)} \le \frac{1}{C_2}$,

$$\begin{aligned}\left|\nabla z^{(j)}\right|(t,\boldsymbol{x}) &\le C_{12}\left(\int_0^t \left|\nabla c^{(j)}\right|(\sigma,\boldsymbol{x})\, d\sigma + |\nabla v_0|(\boldsymbol{x})\right), \\ \left|\nabla z^{(1)} - \nabla z^{(2)}\right|(t,\boldsymbol{x}) &\le C_{12}\int_0^t \left(\left|\nabla z^{(2)}\right|(s,\boldsymbol{x}) + \int_0^t \left|\nabla c^{(1)}\right|(\sigma,\boldsymbol{x})\, d\sigma\right) \\ &\quad \cdot \left|c^{(1)} - c^{(2)}\right|(s,\boldsymbol{x})\, ds \\ &\quad + C_{12}\int_0^t \left|\nabla c^{(1)} - \nabla c^{(2)}\right|(s,\boldsymbol{x})\, ds \qquad (3.28)\end{aligned}$$

are satisfied for $(t,\boldsymbol{x}) \in (0,T)\times\Omega$ and $j \in \{1,2\}$.
Therefore, we have

$$\begin{aligned}\left|v^{(1)} - v^{(2)}\right|(t,\boldsymbol{x}) &= \left|\frac{z^{(2)} - z^{(1)}}{z^{(1)}z^{(2)}}\right|(t,\boldsymbol{x}) \le C_{13}\int_0^t \left|c^{(1)} - c^{(2)}\right|(s,\boldsymbol{x})\, ds, \\ \left|\nabla v^{(1)} - \nabla v^{(2)}\right|(t,\boldsymbol{x}) &= \left|-\frac{\nabla z^{(1)}}{(z^{(1)})^2} + \frac{\nabla z^{(2)}}{(z^{(2)})^2}\right|(t,\boldsymbol{x}) \\ &= \left|\frac{\nabla(z^{(2)} - z^{(1)})}{(z^{(2)})^2} + \frac{((z^{(1)})^2 - (z^{(2)})^2)\nabla z^{(1)}}{(z^{(1)})^2(z^{(2)})^2}\right|(t,\boldsymbol{x}) \\ &\le C_{13}\left[|\nabla v_0|(\boldsymbol{x}) + \int_0^t \left(\left|\nabla c^{(1)}\right| + \left|\nabla c^{(2)}\right|\right)(\sigma,\boldsymbol{x})\, d\sigma\right] \\ &\quad \cdot \int_0^t \left|c^{(1)} - c^{(2)}\right|(s,\boldsymbol{x})\, ds + C_{13}\int_0^t \left|\nabla c^{(1)} - \nabla c^{(2)}\right|(s,\boldsymbol{x})\, ds \qquad (3.29)\end{aligned}$$

for $(t,\boldsymbol{x}) \in (0,T)\times\Omega$.
In particular, by Hölder's inequality this implies

$$\begin{aligned}\int_\Omega \left|v^{(1)} - v^{(2)}\right|^2(t,\boldsymbol{x})\, d\boldsymbol{x} &\le C_{13}^2\int_\Omega t\int_0^t \left|c^{(1)} - c^{(2)}\right|^2(s,\boldsymbol{x})\, ds d\boldsymbol{x} \\ &\le C_{13}^2 t^2 \sup_{s\in(0,t)}\int_\Omega \left|c^{(1)} - c^{(2)}\right|^2(s,\boldsymbol{x}) d\boldsymbol{x}\end{aligned}$$

$$\leq \quad C_{13}^2 T^2 \left\| c^{(1)} - c^{(2)} \right\|^2_{L^\infty(0,t;L^2(\Omega))} \tag{3.30}$$

and

$$\int_0^t \int_\Omega \left| v^{(1)} - v^{(2)} \right|^2 (s, \boldsymbol{x})\, d\boldsymbol{x} ds \leq C_{13}^2 T^2 \int_0^t \left\| c^{(1)} - c^{(2)} \right\|^2_{L^\infty(0,s;L^2(\Omega))} ds \tag{3.31}$$

for $t \in (0,T)$.

In view of (2.5)-(2.7), $L := l^{(1)} - l^{(2)}$ satisfies

$$L_t = \alpha \Delta L - \beta L + \delta_l \left(c^{(1)} v^{(1)} - c^{(2)} v^{(2)} \right) \qquad \text{in } (0,T) \times \Omega \tag{3.32}$$

together with the homogeneous Neumann boundary condition and $L(0, \boldsymbol{x}) = 0$ for $\boldsymbol{x} \in \Omega$. Hence, by [22, Theorem IV.9.1] (and the remark at the end of Section IV.9 concerning the Neumann problem) we obtain

$$\|L\|_{L^2(0,t;W^{2,2}(\Omega))} \leq C_{14} \left\| c^{(1)} v^{(1)} - c^{(2)} v^{(2)} \right\|_{L^2((0,t)\times\Omega)}$$

for all $t \in (0,T)$ and deduce from (3.26) and (3.31) that

$$\begin{aligned} & \left\| l^{(1)} - l^{(2)} \right\|^2_{L^2((0,t)\times\Omega)} + \left\| \nabla l^{(1)} - \nabla l^{(2)} \right\|^2_{L^2((0,t)\times\Omega)} \\ \leq \quad & C_{15} \int_0^t \left\| c^{(1)} - c^{(2)} \right\|^2_{L^\infty(0,s;L^2(\Omega))} ds \end{aligned} \tag{3.33}$$

is fulfilled for all $t \in (0,T)$.
Moreover, by using (3.32), $L(0, \boldsymbol{x}) = 0$ for $\boldsymbol{x} \in \Omega$, (3.26), (3.30) and Young's inequality, we obtain

$$\begin{aligned} \int_\Omega \left| l^{(1)} - l^{(2)} \right|^2 (t, \boldsymbol{x})\, d\boldsymbol{x} \quad &= \quad 2 \int_0^t \int_\Omega L L_t(s, \boldsymbol{x})\, d\boldsymbol{x} ds \\ &= \quad -2\alpha \int_0^t \int_\Omega |\nabla L|^2 (s, \boldsymbol{x})\, d\boldsymbol{x} ds - 2\beta \int_0^t \int_\Omega L^2(s, \boldsymbol{x})\, d\boldsymbol{x} ds \\ &\quad +2\delta_l \int_0^t \int_\Omega L \left(c^{(1)} v^{(1)} - c^{(2)} v^{(2)} \right) (s, \boldsymbol{x})\, d\boldsymbol{x} ds \\ &\leq \quad \frac{\delta_l^2}{2\beta} \int_0^t \int_\Omega \left(c^{(1)} v^{(1)} - c^{(2)} v^{(2)} \right)^2 (s, \boldsymbol{x})\, d\boldsymbol{x} ds \\ &\leq \quad C_{16} \left\| c^{(1)} - c^{(2)} \right\|^2_{L^\infty(0,t;L^2(\Omega))} \end{aligned} \tag{3.34}$$

for $t \in (0,T)$.

Since $\boldsymbol{y}^{(j)}$ is a solution to a linear ODE, we obtain (similarly as done above for $z^{(j)}$) from (3.26), (3.29), and the regularity of $\boldsymbol{G}$ that

$$\left| \boldsymbol{y}_i^{(1)} - \boldsymbol{y}_i^{(2)} \right| (t, \boldsymbol{x}) \leq C_{17} \int_0^t \left(\left| c^{(1)} - c^{(2)} \right| + \left| l^{(1)} - l^{(2)} \right| \right) (s, \boldsymbol{x})\, ds \tag{3.35}$$

holds for $t \in (0,T)$ and $i \in \{1,2\}$. Thus, in a similar manner we have

$$\left|\kappa^{(1)} - \kappa^{(2)}\right|(t,\boldsymbol{x}) \le C_{18} \int_0^t \left(\left|c^{(1)} - c^{(2)}\right| + \left|l^{(1)} - l^{(2)}\right|\right)(s,\boldsymbol{x})\, ds \tag{3.36}$$

for $t \in (0,T)$ due to (3.26), (3.35) and the regularity of H.

Next in order to abbreviate notation we define $\varphi_j := \varphi(\kappa^{(j)}, c^{(j)}, v^{(j)})$, $\psi_j := \psi(\kappa^{(j)}, v^{(j)})$ and $f_j := f(c^{(j)}, l^{(j)})$ for $j \in \{1,2\}$. As $2p \ge 2$ and $c^{(j)}$ is a weak solution to the first equation of (2.5) fulfilling (2.6), (2.7) and (3.26), we deduce that

$$\begin{aligned}
&\frac{1}{2}\int_\Omega \left(c^{(1)} - c^{(2)}\right)^2 (t,\boldsymbol{x}) d\boldsymbol{x} \\
&= \frac{1}{2}\int_0^t \int_\Omega \frac{d}{dt}\left(c^{(1)} - c^{(2)}\right)^2 (s,\boldsymbol{x})\, d\boldsymbol{x} ds \\
&= \int_0^t \int_\Omega \nabla\left(c^{(1)} - c^{(2)}\right)\Big[- \varphi_1 \nabla c^{(1)} + \varphi_2 \nabla c^{(2)} + \psi_1 c^{(1)} \nabla v^{(1)} - \psi_2 c^{(2)} \nabla v^{(2)} \\
&\quad + f_1 c^{(1)} \nabla l^{(1)} - f_2 c^{(2)} \nabla l^{(2)}\Big](s,\boldsymbol{x})\, d\boldsymbol{x} ds \\
&\quad + \int_0^t \int_\Omega \mu_c \left(c^{(1)} - c^{(2)}\right)\left[c^{(1)}\left(1 - \frac{c^{(1)}}{K_c} - \eta_1 \frac{v^{(1)}}{K_v}\right)\right. \\
&\quad \left. - c^{(2)}\left(1 - \frac{c^{(2)}}{K_c} - \eta_1 \frac{v^{(2)}}{K_v}\right)\right](s,\boldsymbol{x})\, d\boldsymbol{x} ds \\
&= -\int_0^t \int_\Omega \varphi_1 \left|\nabla c^{(1)} - \nabla c^{(2)}\right|^2 (s,\boldsymbol{x})\, d\boldsymbol{x} ds \\
&\quad + \int_0^t \int_\Omega \psi_1 c^{(1)} \nabla\left(v^{(1)} - v^{(2)}\right) \nabla\left(c^{(1)} - c^{(2)}\right)(s,\boldsymbol{x})\, d\boldsymbol{x} ds \\
&\quad + \int_0^t \int_\Omega \nabla\left(c^{(1)} - c^{(2)}\right)\Big[(\varphi_2 - \varphi_1)\nabla c^{(2)} + \left(\psi_1 c^{(1)} - \psi_2 c^{(2)}\right)\nabla v^{(2)} \\
&\quad + \left(f_1 c^{(1)} - f_2 c^{(2)}\right)\nabla l^{(2)}\Big](s,\boldsymbol{x})\, d\boldsymbol{x} ds \\
&\quad + \int_0^t \int_\Omega f_1 c^{(1)} \nabla\left(l^{(1)} - l^{(2)}\right)\nabla\left(c^{(1)} - c^{(2)}\right)(s,\boldsymbol{x})\, d\boldsymbol{x} ds \\
&\quad + \int_0^t \int_\Omega \mu_c \left(c^{(1)} - c^{(2)}\right)\left[c^{(1)}\left(1 - \frac{c^{(1)}}{K_c} - \eta_1 \frac{v^{(1)}}{K_v}\right)\right. \\
&\quad \left. - c^{(2)}\left(1 - \frac{c^{(2)}}{K_c} - \eta_1 \frac{v^{(2)}}{K_v}\right)\right](s,\boldsymbol{x})\, d\boldsymbol{x} ds \\
&=: -I_1 + I_2 + I_3 + I_4 + I_5
\end{aligned} \tag{3.37}$$

holds for $t \in (0,T)$.

We further define

$$\begin{aligned}
g(t,\boldsymbol{x}) &:= \left(\left|c^{(1)} - c^{(2)}\right| + \left|l^{(1)} - l^{(2)}\right|\right)(t,\boldsymbol{x}), \\
h(t,\boldsymbol{x}) &:= \left(\left|\nabla c^{(2)}\right| + \left|\nabla v^{(2)}\right| + \left|\nabla l^{(2)}\right|\right)(t,\boldsymbol{x})
\end{aligned} \tag{3.38}$$

for $(t,\boldsymbol{x}) \in (0,T) \times \Omega$.

In view of (3.26)-(3.36), (3.16) and (3.3) there are positive constants ε and C_{19} such that

$$\varphi_1 \geq \varepsilon \qquad \text{in } (0,T)\times\Omega \tag{3.39}$$

and

$$\begin{gathered}\left(|\varphi_1-\varphi_2|+\left|\psi_1 c^{(1)}-\psi_2 c^{(2)}\right|+\left|f_1 c^{(1)}-f_2 c^{(2)}\right|\right)(t,\boldsymbol{x}) \leq C_{19}\left(g(t,\boldsymbol{x})+\int_0^t g(s,\boldsymbol{x})\,ds\right),\\ \|h\|_{L^{2p}((0,t)\times\Omega)} \leq C_{19}\end{gathered} \tag{3.40}$$

are fulfilled for $t\in(0,T)$.

Next we fix

$$r := \frac{2p}{p-1} \qquad \text{and} \qquad a := \frac{\frac{1}{2}-\frac{1}{r}}{\frac{1}{n}} = \frac{n}{2p} \tag{3.41}$$

and remark that $p > \frac{n+2}{2}$ yields $a\in(0,1)$. Therefore, by the inequalities of Gagliardo-Nirenberg and Young, there exist constants $C_{GN}>0$ and $C_\varepsilon>0$ such that

$$\|u\|_{L^r(\Omega)} \leq C_{GN}\left(\|\nabla u\|_{L^2(\Omega)}^a \|u\|_{L^2(\Omega)}^{1-a} + \|u\|_{L^2(\Omega)}\right) \leq \varepsilon\|\nabla u\|_{L^2(\Omega)} + C_\varepsilon\|u\|_{L^2(\Omega)} \tag{3.42}$$

is satisfied for all $u\in W^{1,2}(\Omega)$.

Furthermore, by (3.2) and (3.26) there is $C_{20}>0$ such that $w(t,\boldsymbol{x}) := h(t,\boldsymbol{x})+|\nabla v_0|(\boldsymbol{x})+\int_0^t(|\nabla c^{(1)}|+|\nabla c^{(2)}|)(\sigma,\boldsymbol{x})\,d\sigma$ satisfies

$$\|w\|_{L^{2p}((0,t)\times\Omega)} \leq C_{20} \tag{3.43}$$

for all $t\in(0,T)$.

Thus, (3.29), (3.33), (3.34) and (3.40)-(3.43) along with $a\in(0,1)$ and $p(1-a)=\frac{2p-n}{2}>1$ and the inequalities of Hölder and Young yield

$$\begin{aligned}
I_2+I_3 \;\leq\;& \int_0^t\int_\Omega \psi_1 c^{(1)}\nabla\left(v^{(1)}-v^{(2)}\right)\nabla\left(c^{(1)}-c^{(2)}\right)(s,\boldsymbol{x})d\boldsymbol{x}ds\\
&+C_{19}\int_0^t\int_\Omega\left|\nabla c^{(1)}-\nabla c^{(2)}\right|(s,\boldsymbol{x})\cdot h(s,\boldsymbol{x})\left(g(s,\boldsymbol{x})+\int_0^s g(\sigma,\boldsymbol{x})\,d\sigma\right)d\boldsymbol{x}ds\\
\leq\;& C_{21}\int_\Omega\int_0^t\int_0^s\left|\nabla c^{(1)}-\nabla c^{(2)}\right|(\sigma,\boldsymbol{x})d\sigma\left|\nabla c^{(1)}-\nabla c^{(2)}\right|(s,\boldsymbol{x})dsd\boldsymbol{x}\\
&+C_{21}\int_0^t\int_\Omega\left|\nabla c^{(1)}-\nabla c^{(2)}\right|(s,\boldsymbol{x})\cdot w(s,\boldsymbol{x})\int_0^s g(\sigma,\boldsymbol{x})\,d\sigma d\boldsymbol{x}ds\\
&+C_{19}\int_0^t\int_\Omega\left|\nabla c^{(1)}-\nabla c^{(2)}\right|(s,\boldsymbol{x})\cdot h(s,\boldsymbol{x})\cdot g(s,\boldsymbol{x})\,d\boldsymbol{x}ds\\
\leq\;& C_{21}\int_\Omega\int_0^t\frac{1}{2}\frac{d}{ds}\left(\int_0^s\left|\nabla c^{(1)}-\nabla c^{(2)}\right|(\sigma,\boldsymbol{x})d\sigma\right)^2 dsd\boldsymbol{x}\\
&+C_{21}\int_0^t\int_0^s\left(\int_\Omega\left|\nabla c^{(1)}-\nabla c^{(2)}\right|^2(s,\boldsymbol{x})\,d\boldsymbol{x}\right)^{\frac{1}{2}}\cdot\left(\int_\Omega|w|^{2p}(s,\boldsymbol{x})\,d\boldsymbol{x}\right)^{\frac{1}{2p}}\\
&\cdot\left(\int_\Omega|g|^{\frac{2p}{p-1}}(\sigma,\boldsymbol{x})\,d\boldsymbol{x}\right)^{\frac{p-1}{2p}}d\sigma ds+C_{19}\int_0^t\left(\int_\Omega\left|\nabla c^{(1)}-\nabla c^{(2)}\right|^2(s,\boldsymbol{x})\,d\boldsymbol{x}\right)^{\frac{1}{2}}
\end{aligned}$$

$$
\begin{aligned}
&\cdot \left(\int_\Omega |h|^{2p}(s,\boldsymbol{x})\, d\boldsymbol{x} \right)^{\frac{1}{2p}} \cdot \left(\int_\Omega |g|^{\frac{2p}{p-1}}(s,\boldsymbol{x})\, d\boldsymbol{x} \right)^{\frac{p-1}{2p}} ds \\
\leq\ & C_{21} \int_\Omega \frac{1}{2} \left(\int_0^t \left| \nabla c^{(1)} - \nabla c^{(2)} \right| (s,\boldsymbol{x}) ds \right)^2 d\boldsymbol{x} \\
&+ C_{21} \int_0^t \int_0^s \left(\int_\Omega \left| \nabla c^{(1)} - \nabla c^{(2)} \right|^2 (s,\boldsymbol{x})\, d\boldsymbol{x} \right)^{\frac{1}{2}} \cdot \left(\int_\Omega |w|^{2p}(s,\boldsymbol{x})\, d\boldsymbol{x} \right)^{\frac{1}{2p}} \\
&\cdot \left[\varepsilon \left(\int_\Omega |\nabla g|^2(\sigma,\boldsymbol{x})\, d\boldsymbol{x} \right)^{\frac{1}{2}} + C_\varepsilon \left(\int_\Omega g^2(\sigma,\boldsymbol{x})\, d\boldsymbol{x} \right)^{\frac{1}{2}} \right] d\sigma ds \\
&+ C_{19} C_{GN} \int_0^t \left(\int_\Omega \left| \nabla c^{(1)} - \nabla c^{(2)} \right|^2 (s,\boldsymbol{x})\, d\boldsymbol{x} \right)^{\frac{1}{2}} \cdot \left(\int_\Omega |h|^{2p}(s,\boldsymbol{x})\, d\boldsymbol{x} \right)^{\frac{1}{2p}} \\
&\cdot \left[\left(\int_\Omega |\nabla g|^2(s,\boldsymbol{x})\, d\boldsymbol{x} \right)^{\frac{a}{2}} \cdot \left(\int_\Omega g^2(s,\boldsymbol{x})\, d\boldsymbol{x} \right)^{\frac{1-a}{2}} + \left(\int_\Omega g^2(s,\boldsymbol{x})\, d\boldsymbol{x} \right)^{\frac{1}{2}} \right] ds \\
\leq\ & C_{21} \frac{t}{2} \int_\Omega \int_0^t \left| \nabla c^{(1)} - \nabla c^{(2)} \right|^2 ds d\boldsymbol{x} \\
&+ \varepsilon C_{21} t^{\frac{1}{2}} \int_0^t \left(\int_\Omega \left| \nabla c^{(1)} - \nabla c^{(2)} \right|^2 (s,\boldsymbol{x})\, d\boldsymbol{x} \right)^{\frac{1}{2}} \\
&\cdot \left(\int_\Omega |w|^{2p}(s,\boldsymbol{x})\, d\boldsymbol{x} \right)^{\frac{1}{2p}} \cdot \left(\int_0^s \int_\Omega |\nabla g|^2(\sigma,\boldsymbol{x})\, d\boldsymbol{x} d\sigma \right)^{\frac{1}{2}} ds \\
&+ C_\varepsilon C_{21} T^{\frac{1}{2}} \int_0^t \left(\int_\Omega \left| \nabla c^{(1)} - \nabla c^{(2)} \right|^2 (s,\boldsymbol{x})\, d\boldsymbol{x} \right)^{\frac{1}{2}} \\
&\cdot \left(\int_\Omega |w|^{2p}(s,\boldsymbol{x})\, d\boldsymbol{x} \right)^{\frac{1}{2p}} \cdot \left(\int_0^s \int_\Omega g^2(\sigma,\boldsymbol{x})\, d\boldsymbol{x} d\sigma \right)^{\frac{1}{2}} ds \\
&+ \frac{\varepsilon}{36} \int_0^t \int_\Omega \left| \nabla c^{(1)} - \nabla c^{(2)} \right|^2 (s,\boldsymbol{x})\, d\boldsymbol{x} ds + \frac{\varepsilon}{72} \int_0^t \int_\Omega |\nabla g|^2(s,\boldsymbol{x})\, d\boldsymbol{x} ds \\
&+ C_{22} \int_0^t \left(\int_\Omega |h|^{2p}(s,\boldsymbol{x})\, d\boldsymbol{x} \right)^{\frac{1}{p(1-a)}} \int_\Omega g^2(s,\boldsymbol{x})\, d\boldsymbol{x} ds \\
&+ C_{22} \int_0^t \left(\int_\Omega |h|^{2p}(s,\boldsymbol{x})\, d\boldsymbol{x} \right)^{\frac{1}{p}} \int_\Omega g^2(s,\boldsymbol{x})\, d\boldsymbol{x} ds \\
\leq\ & C_{21} \frac{t}{2} \int_0^t \int_\Omega \left| \nabla c^{(1)} - \nabla c^{(2)} \right|^2 d\boldsymbol{x} ds \\
&+ \varepsilon C_{21} t^{\frac{1}{2}} \left[\left(\int_0^t \int_\Omega \left| \nabla c^{(1)} - \nabla c^{(2)} \right|^2 (\sigma,\boldsymbol{x})\, d\boldsymbol{x} d\sigma \right)^{\frac{1}{2}} \right. \\
&\left. + \left(\int_0^t \int_\Omega \left| \nabla l^{(1)} - \nabla l^{(2)} \right|^2 (\sigma,\boldsymbol{x})\, d\boldsymbol{x} d\sigma \right)^{\frac{1}{2}} \right] \\
&\cdot \left(\int_0^t \int_\Omega \left| \nabla c^{(1)} - \nabla c^{(2)} \right|^2 (s,\boldsymbol{x})\, d\boldsymbol{x} ds \right)^{\frac{1}{2}} \cdot \left(\int_0^t \left(\int_\Omega |w|^{2p}(s,\boldsymbol{x})\, d\boldsymbol{x} \right)^{\frac{1}{p}} ds \right)^{\frac{1}{2}} \\
&+ C_\varepsilon C_{21} T^{\frac{1}{2}} \left(\int_0^t \int_\Omega g^2(\sigma,\boldsymbol{x})\, d\boldsymbol{x} d\sigma \right)^{\frac{1}{2}} \cdot \left(\int_0^t \int_\Omega \left| \nabla c^{(1)} - \nabla c^{(2)} \right|^2 (s,\boldsymbol{x})\, d\boldsymbol{x} ds \right)^{\frac{1}{2}}
\end{aligned}
$$

$$
\begin{aligned}
&\cdot \left(\int_0^t \left(\int_\Omega |w|^{2p}(s,\boldsymbol{x})\, d\boldsymbol{x} \right)^{\frac{1}{p}} ds \right)^{\frac{1}{2}} \\
&+\frac{\varepsilon}{18} \int_0^t \int_\Omega \left| \nabla c^{(1)} - \nabla c^{(2)} \right|^2 (s,\boldsymbol{x})\, d\boldsymbol{x} ds \\
&+\frac{\varepsilon}{36} \int_0^t \int_\Omega \left| \nabla l^{(1)} - \nabla l^{(2)} \right|^2 (s,\boldsymbol{x})\, d\boldsymbol{x} ds \\
&+C_{22} \left(\sup_{s\in(0,t)} \int_\Omega g^2(s,\boldsymbol{x})\, d\boldsymbol{x} \right) \cdot \left(C_{19}^{\frac{2}{1-a}} t^{\frac{p(1-a)-1}{p(1-a)}} + C_{19}^2 t^{\frac{p-1}{p}} \right) \\
\leq\ & \left(C_{21}\frac{t}{2} + \varepsilon C_{21} t^{\frac{1}{2}} \cdot C_{20} t^{\frac{p-1}{2p}} \right) \int_0^t \int_\Omega \left| \nabla c^{(1)} - \nabla c^{(2)} \right|^2 d\boldsymbol{x} ds \\
&+\frac{\varepsilon}{18} \int_0^t \int_\Omega \left| \nabla c^{(1)} - \nabla c^{(2)} \right|^2 d\boldsymbol{x} ds \\
&+\frac{9\varepsilon C_{21}^2 T}{2} \cdot C_{20}^2 T^{\frac{p-1}{p}} \cdot C_{15} \int_0^t \left\| c^{(1)} - c^{(2)} \right\|^2_{L^\infty(0,s;L^2(\Omega))} ds \\
&+\frac{\varepsilon}{18} \int_0^t \int_\Omega \left| \nabla c^{(1)} - \nabla c^{(2)} \right|^2 d\boldsymbol{x} ds \\
&+C_\varepsilon^2 C_{21}^2 T \cdot \frac{9}{2\varepsilon} \cdot C_{20}^2 T^{\frac{p-1}{p}} \cdot (2C_{15}+2) \int_0^t \left\| c^{(1)} - c^{(2)} \right\|^2_{L^\infty(0,s;L^2(\Omega))} ds \\
&+\frac{\varepsilon}{18} \int_0^t \int_\Omega \left| \nabla c^{(1)} - \nabla c^{(2)} \right|^2 d\boldsymbol{x} ds \\
&+\frac{\varepsilon}{36} \cdot C_{15} \int_0^t \left\| c^{(1)} - c^{(2)} \right\|^2_{L^\infty(0,s;L^2(\Omega))} ds \\
&+C_{22} \left(C_{19}^{\frac{4p}{2p-n}} t^{\frac{2p-n-2}{2p-n}} + C_{19}^2 t^{\frac{p-1}{p}} \right) \cdot (2C_{16}+2) \left\| c^{(1)} - c^{(2)} \right\|^2_{L^\infty(0,t;L^2(\Omega))} \\
\leq\ & \left(C_{21}\frac{t}{2} + \varepsilon C_{21} C_{20} t^{\frac{2p-1}{2p}} + \frac{\varepsilon}{6} \right) \int_0^t \int_\Omega \left| \nabla c^{(1)} - \nabla c^{(2)} \right|^2 d\boldsymbol{x} ds \\
&+C_{23} \int_0^t \left\| c^{(1)} - c^{(2)} \right\|^2_{L^\infty(0,s;L^2(\Omega))} ds \\
&+C_{24} \left(t^{\frac{2p-n-2}{2p-n}} + t^{\frac{p-1}{p}} \right) \left\| c^{(1)} - c^{(2)} \right\|^2_{L^\infty(0,t;L^2(\Omega))} \qquad (3.44)
\end{aligned}
$$

for $t \in (0,T)$.

Thus, fixing $t_0 := \min\{\frac{\varepsilon}{3C_{21}}, (6C_{20}C_{21})^{-\frac{2p}{2p-1}}, (8C_{24})^{-\frac{2p-n}{2p-n-2}}, (8C_{24})^{-\frac{p}{p-1}}, T\}$, inserting (3.39) and (3.44) into (3.37) and using Young's inequality along with (3.26), (3.29) and (3.33), we conclude that

$$
\begin{aligned}
&\frac{1}{2} \int_\Omega \left(c^{(1)} - c^{(2)} \right)^2 (t,\boldsymbol{x}) d\boldsymbol{x} \\
&\quad \leq\ -\varepsilon \int_0^t \int_\Omega \left| \nabla c^{(1)} - \nabla c^{(2)} \right|^2 d\boldsymbol{x} ds + \frac{\varepsilon}{2} \int_0^t \int_\Omega \left| \nabla c^{(1)} - \nabla c^{(2)} \right|^2 d\boldsymbol{x} ds \\
&\qquad +C_{23} \int_0^t \left\| c^{(1)} - c^{(2)} \right\|^2_{L^\infty(0,s;L^2(\Omega))} ds + \frac{1}{4} \left\| c^{(1)} - c^{(2)} \right\|^2_{L^\infty(0,t;L^2(\Omega))} \\
&\qquad +\frac{\varepsilon}{2} \int_0^t \int_\Omega \left| \nabla c^{(1)} - \nabla c^{(2)} \right|^2 d\boldsymbol{x} ds + \frac{C_{25}}{\varepsilon} \int_0^t \left\| c^{(1)} - c^{(2)} \right\|^2_{L^\infty(0,s;L^2(\Omega))} ds
\end{aligned}
$$

$$
\begin{aligned}
&+C_{26}\int_0^t \left\|c^{(1)}-c^{(2)}\right\|^2_{L^\infty(0,s;L^2(\Omega))}ds\\
\leq\ & C_{27}\int_0^t \left\|c^{(1)}-c^{(2)}\right\|^2_{L^\infty(0,s;L^2(\Omega))}ds+\frac{1}{4}\left\|c^{(1)}-c^{(2)}\right\|^2_{L^\infty(0,t;L^2(\Omega))}
\end{aligned}
$$

holds for all $t\in(0,t_0)$. As the right-hand side of the last inequality is nondecreasing for $t\in(0,t_0)$, we obtain

$$
\begin{aligned}
\left\|c^{(1)}-c^{(2)}\right\|^2_{L^\infty(0,t;L^2(\Omega))} &= \sup_{s\in(0,t)}\int_\Omega \left(c^{(1)}-c^{(2)}\right)^2(s,\boldsymbol{x})d\boldsymbol{x}\\
&\leq 4C_{27}\int_0^t \left\|c^{(1)}-c^{(2)}\right\|^2_{L^\infty(0,s;L^2(\Omega))}ds
\end{aligned}
$$

for $t\in(0,t_0)$. In view of $c^{(1)}(0,\boldsymbol{x})=c^{(2)}(0,\boldsymbol{x})=c_0(\boldsymbol{x})$, Gronwall's lemma implies that $c^{(1)}=c^{(2)}$ in $[0,t_0]\times\Omega$.

As all the constants depend on T but not on t_0, by repeating this argument we have $c^{(1)}=c^{(2)}$ in $[mt_0,\min\{(m+1)t_0,T\}]\times\Omega$ for all $m\in\mathbb{N}$ such that $mt_0\leq T$. Hence, $c^{(1)}=c^{(2)}$ in $[0,T]\times\Omega$. In view of (3.29)-(3.36), we further deduce that the solutions $(c^{(j)},v^{(j)},l^{(j)},\boldsymbol{y}^{(j)},\kappa^{(j)})$, $j\in\{1,2\}$, to (2.5)-(2.7) coincide. Thus, the proof of the theorem is completed. □

3.2 The case with constant delay

Now we consider the case with a constant delay $\tau>0$ in equation (2.4) for the cell contractivity. We prove the local existence by using the method of steps which is well-known in the context of delay differential equations (see e.g., [3, 4] and the references therein).

Theorem 3.2 *Suppose that $\tau>0$ and $p\in(\frac{n+2}{2},\infty)$ and let* (3.2), (3.3) *and* (2.3) *be fulfilled. Then there exists $T>0$ such that* (2.5)-(2.7) *has a unique solution satisfying* (3.4).

Proof. We take $T>0$ as defined in Theorem 3.1 and set $t_m:=\min\{m\tau,T\}$ for $m\in\mathbb{N}_0$ and $m_0:=\max\{m\in\mathbb{N}_0\,:\,t_m<T\}$. Then, in view of (2.7), $\tilde{\boldsymbol{y}}(t,\boldsymbol{x}):=\boldsymbol{y}(t-\tau,\boldsymbol{x})$ satisfies $\tilde{\boldsymbol{y}}(t,\boldsymbol{x})=\boldsymbol{y}_0(\boldsymbol{x})$ for $(t,\boldsymbol{x})\in[0,t_1]\times\bar{\Omega}$ and therefore fulfills $\tilde{\boldsymbol{y}}\in Z^2\cap V^2$ and $\tilde{\boldsymbol{y}}\in Y$ in $[0,t_1]\times\bar{\Omega}$ due to (3.2).

Hence, (2.4) is a linear ODE in $(0,t_1]\times\Omega$ so that the existence of a unique solution $\boldsymbol{S}^{(1)}:=(c^{(1)},v^{(1)},l^{(1)},\boldsymbol{y}^{(1)},\kappa^{(1)})$ to (2.5)-(2.7) in $[0,t_1]\times\Omega$ satisfying (3.4) is proved in exactly the same way as in Theorem 3.1 (in fact, even statements (3.16), (3.24) and (3.36) concerning κ remain unchanged).

Now assume that we have a solution $\boldsymbol{S}^{(m)}$ to (2.5)-(2.7) in $[0,t_m]\times\Omega$ satisfying (3.4) for some $m\leq m_0$. Then $\tilde{\boldsymbol{y}}\in Z^2\cap V^2$ and $\tilde{\boldsymbol{y}}\in Y$ in $[0,t_{m+1}]\times\bar{\Omega}$ hold due to (3.4). Hence, by Theorem 3.1 there exists a unique solution $\boldsymbol{S}^{(m+1)}$ to (2.5)-(2.7) in $[0,t_{m+1}]\times\Omega$ satisfying (3.4). In view of the uniqueness, we have $\boldsymbol{S}^{(m+1)}=\boldsymbol{S}^{(m)}$ in $[0,t_m]\times\Omega$. By mathematical induction we obtain a unique solution to (2.5)-(2.7) in $[0,T)\times\Omega$ which fulfills (3.4). □

4 Nondimensionalization

Before performing our numerical simulations, we write system (2.5) in terms of dimensionless variables. To this end we rescale

$$\begin{aligned} &\tilde{c} := \frac{c}{K_c}, \quad \tilde{v} := \frac{v}{K_v}, \quad \tilde{l} := \frac{l}{l_0}, \quad \tilde{\boldsymbol{x}} = \frac{\boldsymbol{x}}{L}, \\ &\tilde{t} := \frac{t}{T}, \quad \tilde{y}_1 = \frac{y_1}{R_0}, \quad \tilde{y}_2 = \frac{y_2}{R_0}, \quad \tilde{\theta} = \frac{t}{\chi T}, \end{aligned} \tag{4.1}$$

where L is the reference length scale, T is the reference time unit, l_0 is the reference concentration of proteolytic rests. Since the processes on the subcellular level are much faster than the ones on the macrolevel we set $\tilde{t} = \chi\tilde{\theta}$ where $\chi \in (0,1)$.

After using (2.8) and the transformations (4.1), we obtain the nondimensionalized system for (2.5) as

$$\begin{cases} \tilde{c}_{\tilde{t}} = \nabla\cdot\left(\tilde{D}_c\dfrac{\kappa}{1+\tilde{c}\tilde{v}}\nabla\tilde{c}\right) - \nabla\cdot\left(\dfrac{\tilde{D}_H\kappa\tilde{v}}{1+\tilde{v}}\tilde{c}\nabla\tilde{v}\right) - \nabla\cdot\left(\dfrac{\tilde{D}_k}{1+\tilde{c}\tilde{l}}\tilde{c}\nabla\tilde{l}\right) \\ \qquad +\tilde{\mu}_c\tilde{c}\left(1-\tilde{c}-\eta_1\tilde{v}\right), \\ \tilde{v}_{\tilde{t}} = -\tilde{\delta}_v\tilde{c}\tilde{v} + \tilde{\mu}_v\tilde{v}\left(1-\eta_2\tilde{c}-\tilde{v}\right), \\ \tilde{l}_{\tilde{t}} = \tilde{\alpha}\Delta\tilde{l} + \tilde{\delta}_l\tilde{c}\tilde{v} - \tilde{\beta}\tilde{l}, \\ \dot{\tilde{y}}_1 = \tilde{k}_1(1-\tilde{y}_1-\tilde{y}_2)\tilde{v} - \tilde{k}_{-1}\tilde{y}_1, \\ \dot{\tilde{y}}_2 = \tilde{k}_2(1-\tilde{y}_1-\tilde{y}_2)\tilde{l} - \tilde{k}_{-2}\tilde{y}_2 \\ \dot{\kappa} = -\tilde{q}\kappa + \dfrac{\tilde{M}\tilde{y}_1(\tilde{\theta}-\tilde{\tau})}{1+\tilde{y}_2(\tilde{\theta}-\tilde{\tau})} \end{cases} \tag{4.2}$$

with 'upper dot' denoting the time derivative with respect to $\tilde{\theta}$ and the dimensionless parameters

$$\begin{aligned} &\tilde{D}_c = \frac{D_cT}{L^2}, && \tilde{D}_H = \frac{D_HTK_v}{L^2}, && \tilde{D}_k = \frac{D_kTl_0}{L^2}, && \tilde{\mu}_c = \mu_cT, \\ &\tilde{\delta}_v = \delta_vK_cT, && \tilde{\mu}_v = \mu_vT, \\ &\tilde{\alpha} = \frac{\alpha T}{L^2}, && \tilde{\delta}_l = \frac{K_cK_vT\delta_l}{l_0}, && \tilde{\beta} = \beta T, \\ &\tilde{k}_1 = K_vk_1\chi T, && \tilde{k}_{-1} = k_{-1}\chi T, && \tilde{k}_2 = l_0k_2\chi T, && \tilde{k}_{-2} = k_{-2}\chi T, \\ &\tilde{q} = q\chi T, && \tilde{M} = M\chi T, && \tilde{\tau} = \frac{\tau}{\chi T}. \end{aligned}$$

For the ease of notation we omit the tildes and continue with system (4.2).

5 Numerical Results

In this section we investigate the qualitative behavior of the model via numerical simulations in 1-D. To this end we consider (4.2) with the initial conditions

$$\begin{aligned} c(0,x) &= \exp\left(\frac{-x^2}{\varepsilon}\right), \quad x \in [0,1] \text{ and } \varepsilon > 0, \\ v(0,x) &= 1 - \exp\left(\frac{-x^2}{\varepsilon}\right), \quad x \in [0,1] \text{ and } \varepsilon > 0, \\ l(0,x) &= \zeta c(x,0), \qquad x \in [0,1] \text{ and } \zeta \in [0,1), \end{aligned} \tag{5.1}$$

for the cancer cell density, ECM density, and concentration of proteolytic residuals, respectively. We assume that initially the space is mainly occupied by the ECM, while there is a cluster of cancer cells which have already penetrated a short distance into the tissue. The initial density of proteolytic rests is proportional to the initial cancer cell density. Throughout our numerical simulations we take $\varepsilon = 0.01$, $\zeta = 0.3$, and impose homogeneous Neumann boundary conditions as in equation (2.6), hence we assume that there is no flux of tumor cells, ECM fibers and proteolytic residuals across the boundary of the domain $\Omega = (0,1)$.
On the subcellular level we expect the concentration y_1 of the integrins binding to ECM fibers to increase on the left side of the domain (due to the high concentration of fibers) and to decrease on the rest of the domain (as cancer cells have not reached that portion yet). On the other hand, the initial concentration y_2 of integrins binding to the soluble ligand originating from proteolysis depends on the initial densities of c and l and thus should decrease throughout the spatial domain. Hence, we choose a gamma probability density function for y_1, whereas for the initial y_2 we take a function with a decaying exponential profile (see Figure 1). Moreover, since contractivity is mainly the outcome of biochemical processes initiated by the binding of integrins to the ECM fibers, we consider κ_0 to be proportional to $y_1(0)$.

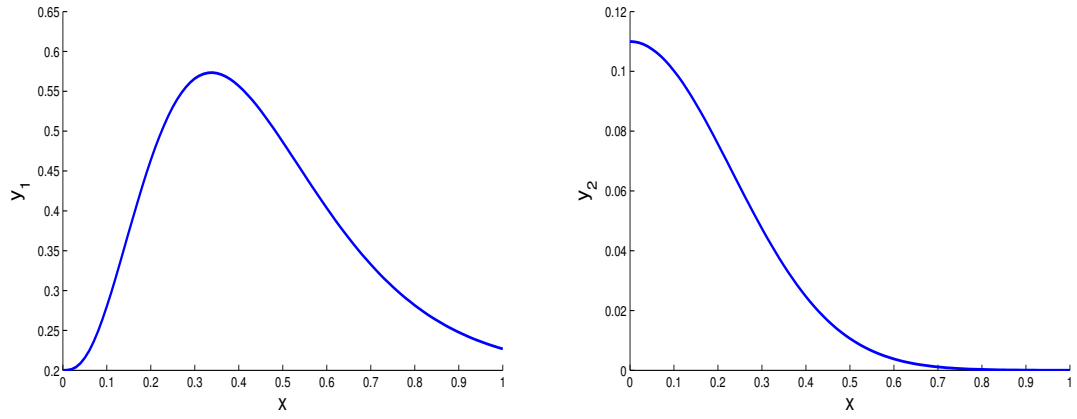

(a) (b)

Figure 1: Initial condition for the vector $\boldsymbol{y}$ of bound integrins

For the discretization of the model we use the finite difference method (FDM). We divide the space interval $[0,1]$ into k parts with $k+1$ nodes, with the space step Δx (in our computations $\Delta x = 0.01$). We start solving system (4.2) with the equation for the ECM

density v. We use forward differences for the time derivatives in our system which after the discretization of the ECM equation leads to

$$v_i^{n+1} = \frac{1}{1+\delta_v c_i^n \overline{\Delta t}}[v_i^n + \overline{\Delta t}\mu_v v_i^n(1-\eta_2 c_i^n - v_i^n)], \quad i = 0,1,2,...,k, \tag{5.2}$$

with n denoting the time level. We choose the time increment for the macrolevel as $\overline{\Delta t} = \chi \Delta t$, where $\Delta t = 0.01$ is the time step for the events on the microscale. In our computations we use $\chi = 0.01$.
In order to discretize the diffusion term on the right-hand side of the equation for proteolytic residuals, we use the central difference and obtain

$$\frac{l_i^{n+1} - l_i^n}{\overline{\Delta t}} = \alpha \cdot \frac{l_{i-1}^{n+1} - 2l_i^{n+1} + l_{i+1}^{n+1}}{(\Delta x)^2} + \delta_l c_i^n v_i^{n+1} - \beta l_i^{n+1}, \quad i = 0,1,...,k. \tag{5.3}$$

leading to the $(k+1)\times(k+1)$ linear system of equations

$$\mathbf{A}_l \mathbf{l}^{n+1} = \mathbf{l}^n + \tilde{\boldsymbol{\vartheta}}_l^{\tilde{n}}, \tag{5.4}$$

where $\mathbf{l}^{n+1}$ is the vector containing the values of l for the $k+1$ space nodes at (n+1)-th time level, $\mathbf{A}_l$ is the tridiagonal matrix coming from the FDM discretization and $\tilde{\boldsymbol{\vartheta}}_l^{\tilde{n}}$ is the vector with the entries $\overline{\Delta t}\delta_l c_i^n v_i^{n+1}$ for $i = 0,1,2,...,k$ where we make use of the updated values v_i^{n+1} found by solving (5.2).
Before solving the equation for the evolution of cancer cell density, we solve the ODEs on the microlevel in order to update the values for the contractivity κ. The corresponding system of delay differential equations is discretized by using the semi-implicit Euler method:

$$\begin{aligned}
(y_1^{n+1})_i &= \frac{1}{1+k_{-1}\Delta t + k_1 v_i^{n+1}\Delta t}[(y_1^n)_i + k_1\Delta t(1-(y_2^n)_i)v_i^{n+1}], \\
(y_2^{n+1})_i &= \frac{1}{1+k_{-2}\Delta t + k_2 l_i^{n+1}\Delta t}[(y_2^n)_i + k_2\Delta t(1-(y_1^{n+1})_i)l_i^{n+1}], \\
\kappa_i^{n+1} &= \frac{1}{1+q\Delta t}\left[\kappa_i^n + \frac{\Delta t M(\widehat{y}_1)_i}{1+(\widehat{y}_2)_i}\right],
\end{aligned} \tag{5.5}$$

where $(\widehat{y}_m)_i$, is the vector containing the values of y_m $(m = 1,2)$ at the space node i $(i = 0,1,2,...k)$ and at time $(n+1)\Delta t - \tau$, with τ denoting the delay.
For the discretization of the PDE for cancer cells we use a nonstandard finite difference scheme [27, 10, 26] which handles the diffusion part explicitly and the reaction terms implicitly. While adapting the method into the first three terms on the right-hand side of the first equation in (4.2) we handle the diffusion, haptotaxis, and chemotaxis coefficients explicitly (w.r.t c) and the rest implicitly:

$$\begin{aligned}
\nabla(\varphi(\kappa,c,v)\nabla c)|_{x_i} &= \frac{1}{2(\Delta x)^2}\sum_{k\in N_i}(\varphi(\kappa_k^{n+1},c_k^n,v_k^{n+1}) + \varphi(\kappa_i^{n+1},c_i^n,v_i^{n+1}))(c_k^{n+1} - c_i^{n+1}), \\
\nabla(\psi(\kappa,v)c\nabla v)|_{x_i} &= \frac{1}{2(\Delta x)^2}\sum_{k\in N_i}(\psi(\kappa_k^{n+1},v_k^{n+1})c_k^{n+1} + \psi(\kappa_i^{n+1},v_i^{n+1})c_i^{n+1}) \\
&\quad \cdot(v_k^{n+1} - v_i^{n+1}),
\end{aligned}$$

$$\nabla(f(c,l)c\nabla l)|_{x_i} = \frac{1}{2(\Delta x)^2}\sum_{k\in N_i}(f(c_k^n,l_k^{n+1})c_k^{n+1}+f(c_i^n,l_i^{n+1})c_i^{n+1})(l_k^{n+1}-l_i^{n+1}), \quad (5.6)$$

where $N_i = \{i-1, i+1\}$ is the index set pointing at the direct neighbors of the node x_i. After employing (5.6) for the discretization of the equation for cancer cells we get

$$\mathbf{A}_c\mathbf{c}^{n+1} = \mathbf{c}^n + \tilde{\boldsymbol{\vartheta}}_c^{\tilde{n}}, \quad (5.7)$$

with the $(k+1)\times(k+1)$ tridiagonal matrix $\mathbf{A}_c$ and the vector $\tilde{\boldsymbol{\vartheta}}_c^{\tilde{n}}$ of length $k+1$ which has entries $\overline{\Delta t}\mu_c(1-c_i^n-\eta_1 v_i^{n+1})$ for $i=0,1,2,...,k$.
In our simulations we fixed the following parameters:

$$\begin{array}{lllll} D_c = 10^{-3}, & D_H = 1, & D_k = 0.5, & \mu_c = 1, & \eta_1 = 0.05, \\ \delta_v = 10, & \mu_v = 0.3, & \eta_2 = 0.9, & \alpha = 1, & \delta_l = 0.05, \quad \beta = 0.15, \\ k_1 = 2, & k_{-1} = 0.06, & k_2 = 0.31, & k_{-2} = 0.048, & q = 3, \quad M = 1, \end{array}$$

which are chosen from the parameter ranges given in Table 1.

Parameters	**Range**	**Source**
D_c (Diffusion coefficient for c)	$10^{-5} - 10^{-3}$	[9]
D_H (Haptotaxis coefficient)	$10^{-3} - 1$	consistent with [9]
D_k (Chemotaxis coefficient)	$10^{-3} - 1$	consistent with [9]
μ_c (Proliferation of cancer cells)	$0.05 - 2$	[9]
δ_v (Rate of degradation of ECM)	1-20	[9]
μ_v (Proliferation of ECM)	0.15-2.5	[9]
α (Diffusion coefficient for l)	$0.001 - 1$	[9]
β (Decay of l)	$0.13 - 0.95$	[9]
δ_l (Production rate of l)	$0.05 - 1$	[9]
k_2 (association rate constant for y_2)	$3\times10^{-1} - 1$	consistent with [11]
k_{-2} (dissociation rate constant for y_2)	$4\times10^{-2} - 10^{-1}$	consistent with [11]

Table 1: Parameter ranges in the model

We illustrate the variations of the cancer cell density, ECM density, concentration of proteolytic rests, and contractivity function in space. As mentioned in Section 2, the cell contractivity is the outcome of a sequence of biochemical processes and thus we introduce a delay (τ) in our system characterizing the time elapsed between integrin binding and the reorganization of the cell's shape by contractivity. In order to see the effect of the delay we draw the set of plots in Figure 2. We show the evolution of cancer cells, ECM fibers, protelytic rests, and contractivity function at different times with a time lag $\tau = 4$ and respectively without delay. As expected, the invasion of cancer cells is faster in the case without delay.
Still in the case with a time lag of $\tau = 4$, we are now interested in the effects of including subcellular dynamics. To this aim we compare the pure macroscopic setting (hence $\kappa = 1$) with our multiscale model (4.2). The simulations are shown for a sequence of time steps in Figure 3. Observe that accounting for the subcellular dynamics slows down the invasion of tumor cells into the tissue, but leads at later times to higher peaks of the aggregates at the invasion front. This is what one would expect from a qualitative point of view, too.

The genuinely macroscopic setting also seems to exacerbate the tissue degradation, while the two settings do not appear to make any difference to the concentration of proteolytic enzymes. Furthermore, notice that ignoring the microscale predicts a decrease in the original tumor, which is actually not expected in practice.

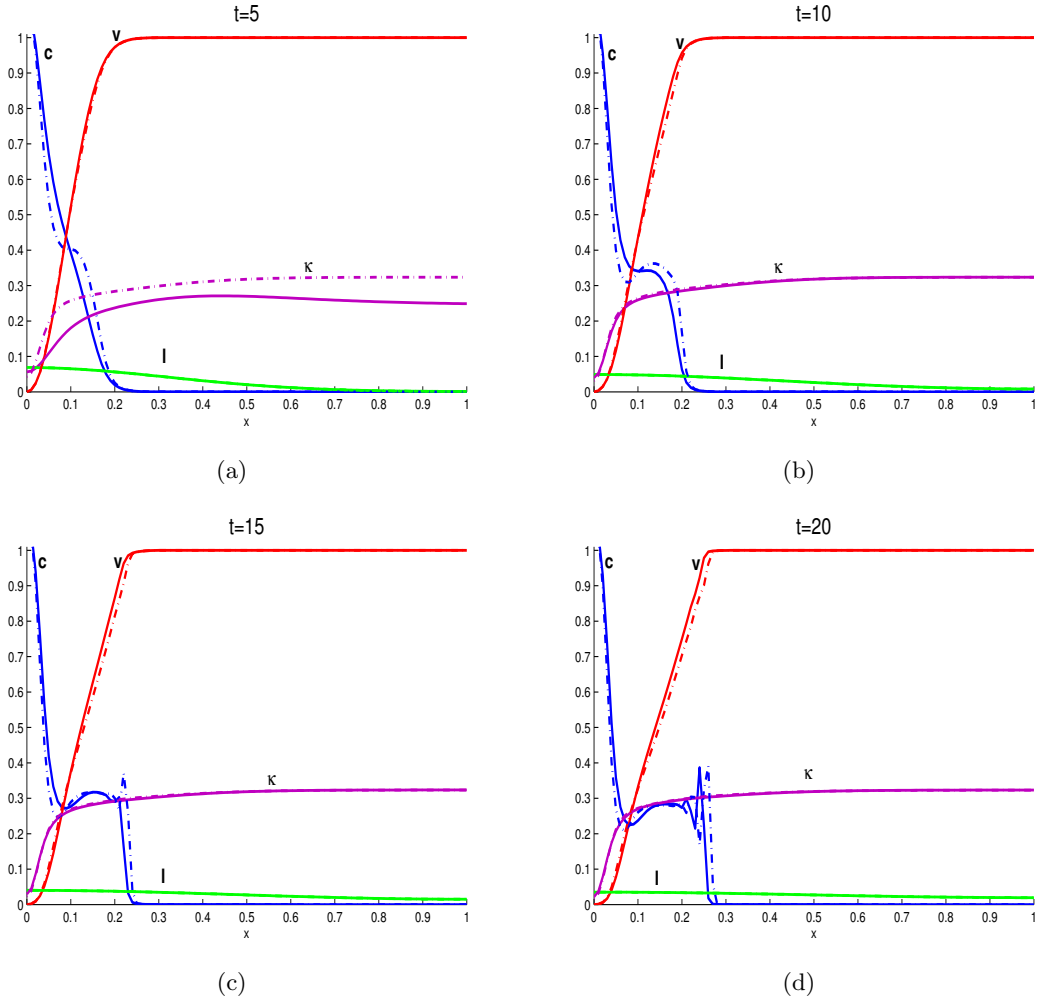

Figure 2: Evolution of tumor cell density (blue), ECM fiber density (red), concentration of proteolytic rests (green), and contractivity function (purple) in the cases with $\tau = 0$ (dash-dot line) and with $\tau = 4$ (solid line).

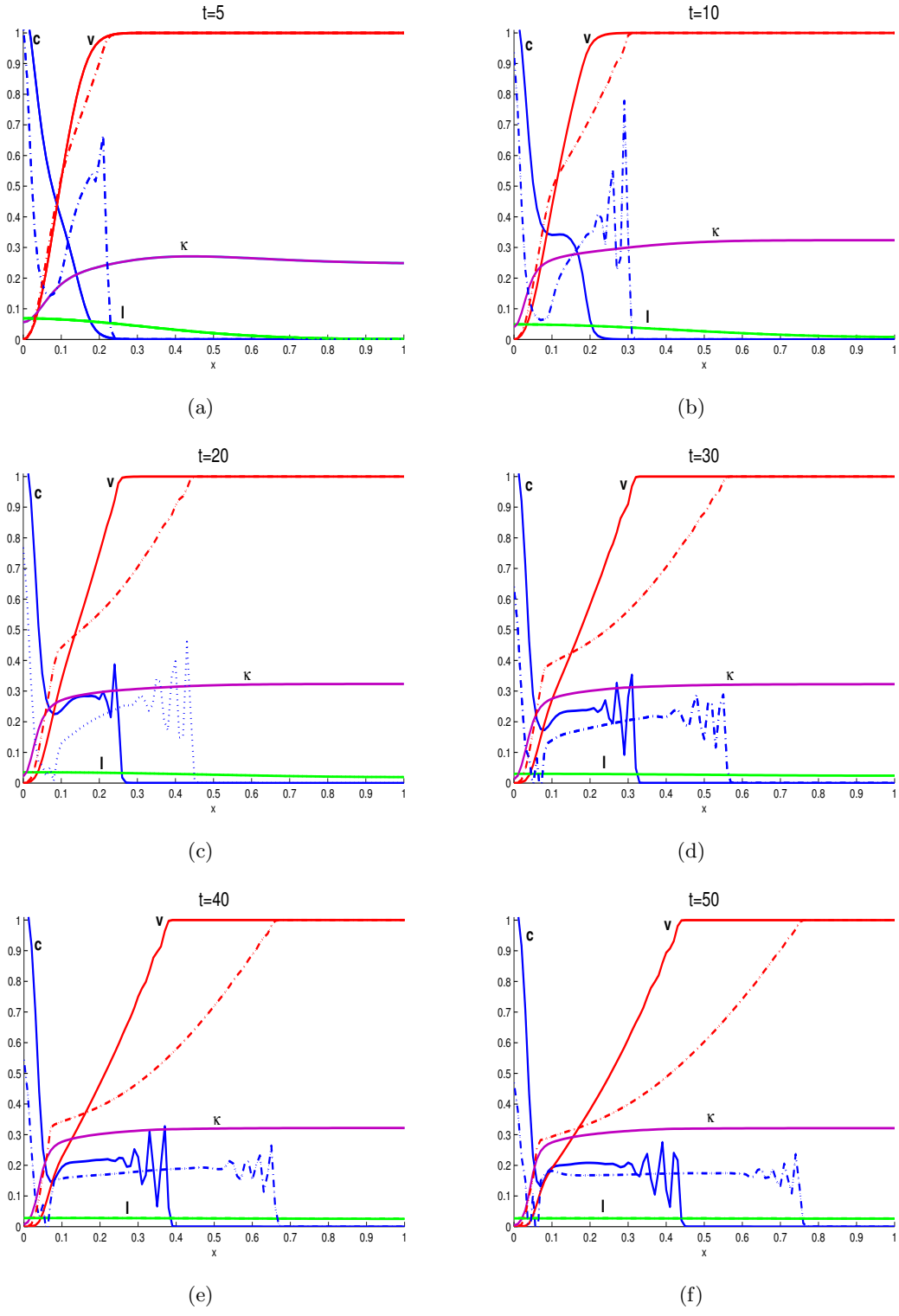

(a) (b) (c) (d) (e) (f)

Figure 3: Evolution of tumor cell density (blue), ECM fiber density (red), concentration of proteolytic rests (green), and contractivity function (purple) in the pure macroscopic setting (dash-dot line) and with κ (solid line) satisfying the last equation in (4.2).

6 Discussion

In this work we proposed and analyzed a mathematical model for tumor cell migration through tissue networks, influenced both by haptotaxis and chemotaxis. Our multiscale setting is connecting the macroscopic level of cell population, fiber density, and chemoattractant concentration with the microscopic one of integrin binding dynamics. The coupling is realized with the aid of a contractivity function involved in the diffusion and haptotaxis coefficients of the cancer cell equation written on the macroscale. The time lag between integrin binding and translation of the initiated signal into motile behavior of the cell population is accounted for via a delay term in the equation for the contractivity function. The multiscality and the coupling between different types of equations increase the complexity of the resulting system, for which we proved the (local) existence of a unique solution. Due to the lack of a priori bounds for the cancer cell density, the global existence result is still out of reach unless generous assumptions are made on the problem's data, which, however, are usually not satisfied in the framework of a concrete biological problem inferring a large variety of fluctuations.
But including microscale dynamics is not only interesting from a mathematical point of view; it can help gaining a deeper insight into the processes involved in and influenced by tumor cell migration. Hence, the cell-ECM interaction modeled by integrin dynamics as in (2.4) has been found to play a crucial role in explaining fingering patterns for glioma [12] in a micro-meso setting, while in the context of bacterial motion the intracellular excitation-adaptation mechanism was shown to influence the motile, aggregation or tactic behavior of the corresponding cell population, see, e.g., [34, 32]. The model proposed in [26] in order to assess the effects of heat shock proteins (HSP) on tumor invasion also aligns to the micro-macro approach proposed in this work, however, it provides a much simplified, rather phenomenological description of the events on the subcellular level connected to HSP dynamics.
The numerical simulations and the comparisons performed in Section 5 illustrate the effects of introducing the microscopic dynamics: the 'classical', purely macroscopic diffusion-haptotaxis-chemotaxis model overestimates the effective distance invaded in the tissue by the cancer cells and underestimates the peaks of their aggregates at the front of the invasion for later times. Furthermore, that setting predicts a decrease in the original tumor, which seems unrealistic from a biological point of view.
Finally, we would like to stress out that the model presented here is merely a paradigm for further multiscale settings, in which enhanced attention can be paid to a more detailed description of subcellular events and hence to their effects on the population spread. The validation of the model predictions would be desirable, which calls for the availability of adequate medical data.

Acknowledgement

G.M. acknowledges the support of LLP Erasmus Staff Mobility Programme during her visit to Technische Universität Kaiserslautern in 24.06.-02.08. 2013.

References

[1] Adams, J.C., *Regulation of protrusive and contractile cell-matrix contacts*, J. Cell Sci. **115** (2002), 257-265.

[2] Anderson, A.R.A., Chaplain, M.A.J., Newman, E.L., Steele, R.J.C., and Thompson, A.M., *Mathematical modeling of tumor invasion and metastasis*, J. of Theoretical Medicine **2** (2000), 129-154.

[3] Banks, H.T., and Musante, C.J., *Well-posedness for a class of abstract nonlinear parabolic systems with time delay*, Nonlinear Analysis **35** (1999), 629-648.

[4] Bellman, R., and Cooke, K.L., *Differential-difference equations*, Academic Press, New York-London, 1963.

[5] Bellomo, N., Bellouquid, A., Nieto, J., and Soler, J., *On the asymptotic theory from microscopic to macroscopic growing tissue models: an overview with perspectives*, Math. Models Methods Appl. Sci. **22** (2012), no.1, 1130001, 37 pages.

[6] Berry, H., *Oscillatory behavior of a simple kinetic model for proteolysis during cell invasion*, Biophys. J. **77** (1999), 655-665.

[7] Carter, S.B., *Haptotaxis and the mechanism of cell motility*, Nature **213** (1967), 256-260.

[8] Chalub, F.A.C.C., Markowich, P.A., Perthame, B., and Schmeiser, C., *Kinetic models for chemotaxis and their drift-diffusion limits*, Monatsh. Math. **142** (2004), 123-141.

[9] Chaplain, M.A., and Lolas, G., *Mathematical modelling of cancer invasion of tissue: dynamic heterogeneity*, Networks and Heterogeneous Media **1** (2006), 399-439.

[10] Eberl, H.J., and Demaret, L., *A finite difference scheme for a degenerated diffusion equation arising in microbial ecology*, Electronic Journal of Differential Equations, Conference 15 (2007), 77-95.

[11] Eladdadi, A., and Isaacson, D., *A mathematical model for the effects of HER2 overexpression on cell proliferation in breast cancer*, Bulletin of Mathematical Biology **70** (2008), 1707-1729.

[12] Engwer, C., Hillen, T., Knappitsch, M.P., and Surulescu, C., *A multiscale model for glioma growth: Formal diffusion limit and application to diffusion tensor imaging data*, preprint WWU Münster (2013).

[13] van der Flier, A., and Sonnenberg, A., *Function and interactions of integrins*, Cell Tissue Res. **305** (2001), 285-298.

[14] Friedl, P., and Wolf, K., *Tumour-cell invasion and migration: diversity and escape mechanisms*, Nature Rev. Cancer **3** (2003), 362-374.

[15] Friedl, P., and Wolf, K., *Proteolytic and non-proteolytic migration of tumour cells and leucocytes*, Biochem. Soc. Symp. **70** (2003), 277-285.

[16] Gatenby, R.A., and Gawlinski, E.T., *A reaction-diffusion model of cancer invasion*, Cancer Res. **56** (1996), 5745-5753.

[17] Hillen, T., *M^5 mesoscopic and macroscopic models for mesenchymal motion*, J. Math. Biol. **53** (2006), 585-616.

[18] Hood, J.D., and Cheresh, D.A., *Role of integrins in cell invasion and migration*, Nature Rev. Cancer **2** (2002), 91-100.

[19] Huttenlocher, A., and Horwitz A.R., *Integrins in cell migration*, Cold Spring Harb. Perspect. Biol. **3** (2011), a005074.

[20] Kelkel, J., and Surulescu, C., *On some models for cancer cell migration through tissue networks*, Math. Biosciences and Engineering **8** (2011), 575-589.

[21] Kelkel, J., and Surulescu, C., *A multiscale approach to cell migration in tissue networks*, Math. Models Methods in Appl. Sci. **22** (2012), no.3, 1150017, 25 pages.

[22] Ladyženskaja, O.A., Solonnikov, V.A., and Ural'ceva N.N., *Linear and quasi-linear equations of parabolic type*, Translations of Mathematical Monographs, Vol. 23, Amer. Math. Soc., Providence, 1968.

[23] Legate, K.R., Wickström, S.A., and Fässler, R., *Genetic and cell biological analysis of integrin outside-in signaling*, Genes Dev. **23** (2009), 397-418.

[24] Lin, B., Holmes, W.R., Wang, C.J., Ueno, T., Harwell, A., Edelstein-Keshet, L., Inoue, T., and Levchenko, A., *Synthetic spatially graded Rac activation drives cell polarization and movement*, PNAS **109** (2012), E3668-E3677.

[25] Lorenz, T., and Surulescu, C., *On a class of multiscale cancer cell migration models: well-posedness in less regular function spaces*, preprint TU Kaiserslautern (2013).

[26] Meral, G., and Surulescu, C., *Mathematical modelling, analysis and numerical simulations for the influence of heat shock proteins on tumour invasion*, J. Math. Anal. Appl. (2013), http://dx.doi.org/10.1016/j.jmaa.2013.06.017

[27] Mickens, R.E., *Nonstandard finite difference schemes*, in Mickens R. E. (ed), Applications of nonstandard finite difference schemes, World Scientific, Singapore, 2000.

[28] Othmer, H.G., Dunbar, S.R., and Alt, W., *Models of dispersal in biological systems*, J. Math. Biol. **26** (1988), 263-298.

[29] Othmer, H., and Hillen, T., *The diffusion limit of transport equations II: chemotaxis equations*, SIAM J. Appl. Math. **62** (2002), 1222-1250.

[30] Surulescu, C., and Surulescu, N., *A nonparametric approach to cell dispersal*, Int. J. Biomath. Biostat. **1** (2010), 109-128.

[31] Surulescu, C., and Surulescu, N., *Modeling and simulation of some cell dispersion problems by a nonparametric method*, Math. Biosc. Eng. **8** (2011), 263-277.

[32] Surulescu, C., and Surulescu, N., *Some classes of stochastic differential equations as an alternative modeling approach to biomedical problems*, in: Kloeden, P.E., and Pötzsche, C. (eds.), Random and Nonautonomous Dynamical Systems in the Life Sciences, LNM Biomathematics Subseries. Springer, Heidelberg, to appear in 2013.

[33] Temam, R., *Navier-Stokes equations. Theory and numerical analysis*, Studies in Mathematics and its Applications, Vol. 2, North-Holland, Amsterdam, 1977.

[34] Xue, C., and Othmer, H.G., *Multiscale models of taxis-driven patterning in bacterial populations*, SIAM J. Appl. Math. **70** (2009), 133-167.